CRP1, a protein localized in filopodia of growth cones, is involved in spinal cord regeneration in adult zebrafish

Running title: CRP1 is involved in spinal cord regeneration

Liping Ma[1], Jeffrey A. Greenwood[2], Ronald P. Hart[1] and Melitta Schachner[1]*

[1] W. M. Keck Center for Collaborative Neuroscience and Department of Cell Biology and Neuroscience, Rutgers, The State University of New Jersey, 604 Allison Road, Piscataway, New Jersey 08854, USA

[2] Department of Biochemistry and Biophysics, Oregon State University, 2011 ALS, Corvallis, OR 97331-7305

* To whom correspondence should be addressed:

Melitta Schachner

W. M. Keck Center for Collaborative Neuroscience,

604 Allison Road, Piscataway, NJ 08854, USA

Tel. +1-732-445-1780

Fax. +1-732-445-2063

schachner@biology.rutgers.edu

Number of figures and tables: 7

Contents of supplemental material: Supplemental Figure S1, S2, S3, S4

Number of pages: 56

Number of words in Abstract: 238

Number of words in Introduction: 488

Number of words in Discussion: 1419

Key words: CRP1, spinal cord, regeneration, zebrafish, Ca^{2+}, filopodia

Acknowledgements

We are grateful to R. Maurer, M. E. Greenberg, R. Goodman, M. Laiho, B. L. Firestein, A. R. Means and Y. Wang for kindly providing plasmids, S.-C. Hsu and K. M. Gibbs for helpful comments on the manuscript. We also thank Brian Siwek for his diligent care of fish. This work was supported by a grant from the New Jersey Commission on Spinal Cord Research [05-3048-SCR-E-0 to M.S.]. M.S. is a consultant at the Center for Neuroscience of Shantou University Medical College.

Abstract

Unlike mammals, adult zebrafish have the ability to regrow descending axons and gain locomotor recovery after spinal cord injury (SCI). One of the decisive factors for successful spinal cord regeneration is the inherent ability of some neurons to regrow their axons via (re)expressing growth associated genes during the regeneration period. The nucleus of the medial longitudinal fascicle (NMLF) is one of several nuclei capable of regenerative response after SCI. Using microarray analysis with laser capture microdissected NMLF, we show that cysteine and glycine-rich protein 1 (CRP1), whose function is largely unknown in the nervous system, is upregulated after SCI. *In vivo* knock-down of CRP1 using an antisense morpholino oligonucleotide impaired axon regeneration and locomotor recovery when compared to a control morpholino, demonstrating that CRP1 upregulation is an important part of the innate regeneration capability in injured neurons of adult zebrafish. In cultured rat hippocampal neurons, endogenous CRP1 accumulated in filopodia of growth cones, and knock-down of CRP1 reduced dendritic, but not axonal outgrowth. Overexpression of CRP1 increased neurite branching and filopodia formation, which requires CRP1 actin-bundling activity. Moreover, Ca^{2+} influx upregulates CRP1 expression in hippocampal neurons, mediated by CaMKIV and CREB. Furthermore, CRP1 is required for the dendritic growth induced by Ca^{2+} influx or CaMKIV. Together, this study is the first to demonstrate the function of CRP1 in the nervous system, its requirement for zebrafish spinal cord regeneration, and its role in neurite remodeling in rat hippocampal neurons.

Introduction

Adult zebrafish, unlike mammals, have the innate ability to regenerate descending axons after spinal cord injury (SCI) leading to locomotor recovery. In addition to a permissive extracellular environment for axon regeneration in zebrafish, the other crucial factor contributing to successful axon regeneration is the inherent ability of some neurons to (re)express growth associated genes and regrow their axons (Becker et al., 1997; Bernhardt, 1999; Becker et al., 2004; Becker and Becker, 2008). *In vivo* depletion of one of these genes, L1.1, dramatically impairs axon regeneration and locomotor recovery (Becker et al., 2004). The ability to upregulate growth associated genes during the regeneration period makes the adult zebrafish a valuable model for identifying molecules involved in successful spinal cord regeneration that can be translated to adult mammals.

The nucleus of medial longitudinal fascicle (NMLF), an anatomically well defined nucleus, is one of several nuclei exhibiting a regenerative response after SCI as evidenced by the upregulation of growth associated genes and axonal regrowth (Becker et al., 1997; Becker et al., 1998; Becker et al., 2004). To investigate the molecular mechanisms underlying this successful regeneration response, we performed microarray analysis with laser capture microdissected NMLF from control or spinal cord lesioned animals. The list of upregulated genes included known growth associated genes such as GAP43 and L1.1, as well as novel genes whose role in axon regeneration are uncharacterized, such as the cysteine and glycine-rich protein 1 (CRP1).

CRP1 belongs to the CRP family, which is a subgroup of LIM-domain proteins in vertebrates and includes CRP1, CRP2, and CRP3/MLP (Louis et al., 1997). CRP1 is

involved in many different cellular functions, acting as a transcriptional cofactor (Chang et al., 2003), suppressing cell proliferation, protecting cells from stress-induced death (Latonen et al., 2008), regulating cell movement during zebrafish development (Miyasaka et al., 2007), and promoting neointima formation (Lilly et al., 2010). CRP1 localizes to the nucleus and actin cytoskeleton, and interacts with α-actinin (Pomies et al., 1997) and cytoskeleton associated protein zyxin (Sadler et al., 1992; Schmeichel and Beckerle, 1998). It has also been demonstrated that CRP1 regulates actin filament bundling via direct interaction with actin (Tran et al., 2005; Jang and Greenwood, 2009). Among the CRP proteins, CRP1 is the only family member that is expressed in the mammalian central nervous system (CNS) (Jain et al., 1998). However, little is known about the physiological function of CRP1 in the CNS.

In the present study, we report that CRP1 is upregulated after SCI in zebrafish and is essential for successful axonal regrowth and locomotor recovery. In cultured rat hippocampal neurons, we show that endogenous CRP1 accumulates in filopodia of growth cones and that knock-down of CRP1 reduces dendritic growth. Moreover, CRP1 is upregulated by Ca^{2+} influx into neurons and is involved in Ca^{2+}-dependent dendritic growth. Our data identify CRP1 as a key component of functional spinal cord regeneration in adult zebrafish and provide the first functional characterization of CRP1 in the CNS.

Materials and Methods

Spinal cord injury in adult zebrafish. Male adult zebrafish (Danio rerio, age > 6 months) were purchased from Aquatica Tropicals Inc. (Plant City, FL). The fish were kept on a 14-hour light and 10-hour dark cycle at 28°C.

Spinal cord injury (SCI) was performed as described (Becker et al., 1997; Becker et al., 2004). In brief, fish were immersed in 0.033% aminobenzoic acid ethylmethylester (MS222; Sigma, St. Louis, MO) for 5 min. After a longitudinal incision was made to expose the vertebral column, a complete transection of the spinal cord was performed between two vertebrae, about 1 mm (for microarray analysis and *in situ* hybridization) or 4 mm (for morpholino treatment) caudal to the brainstem-spinal cord junction, corresponding to the second and eighth vertebra respectively. The number of animals used for each experiment can be found in figure legends. The sham-lesioned control had identical surgical procedures except that the spinal cord was not cut (referred to as control). The wound was sealed with Histoacryl (B. Braun, Melsungen, Germany).

All animal experiments were carried out according to a protocol approved by the Rutgers University Animal Care Committee, which conformed to NIH guidelines.

Laser capture microdissection, RNA isolation and amplification. A photoablation and laser microdissection system (PALM, Carl Zeiss, Thornwood, NY) was used as previously described (Liss et al., 2005). At 11 days after SCI, the brain was removed, embedded in Tissue-Tek OTC, and snap frozen in isopentane (cooled on dry ice). According to the atlas of zebrafish brain (Wullimann, 1996), coronal cryosections (20 μm) of zebrafish brainstem containing NMLF (approximately 30 sections) were cut and

mounted on RNase-free, ultraviolet light-treated, and poly-L-lysine coated membrane slides (1 mm polyethylene-naphthalate membrane, PALM). Sections were fixed with ethanol (four washes with 70%, 95%, 100% ethanol, respectively) and stained with 1% cresyl violet in 100% ethanol, and dried. The NMLF area was cut and captured directly into an adhesive cap (PALM). The buffer RLT (RNeasy Micro Kit; Qiagen, Hilden, Germany) supplemented with β-mercaptoethanol (10 μl/ml) was added into the tube which was then incubated upside-down for 30 min at room temperature. Each condition (control or SCI) consisted of three microarrays. The RNA sample for each microarray was prepared from NMLF tissues pooled from 3 animals.

Total RNA was isolated using the RNeasy Micro Kit (Qiagen) according to the manufacturer's directions with the addition of linear acrylamide (Ambion, Austin, TX) as RNA carrier to the lysate. Then, the RNA was amplified using the RampUP RNA amplication kit (Genisphere, Hatfield, PA) as described in the Genisphere RampUP product manual.

Microarray analysis and quantitative real-time PCR. Affymetrix GeneChip® Zebrafish Genome Arrays (Affymetrix, Santa Clara, CA) containing probes for 14,900 transcripts were used for gene expression analysis, according to the manufacturer's instructions. Complementary DNA was reverse transcribed from the amplified RNA, and hybridized to microarrays. Following hybridization, the arrays were washed and scanned following standard Affymetrix protocols. Data were extracted from CEL files using the RMA method (Irizarry et al., 2003) as implemented in Gene Traffic (Iobion). Differences between microarray results from lesioned and sham-lesioned animals (n=3 microarrays

per group) were compared using Welch's *t*-test using the Benjamini-Hochberg FDR to estimate multiple measurement errors.

Quantitative real-time polymerase chain reaction (qPCR) was performed with Power SYBR Green PCR Master Mix (Applied Biosystems, Foster City, CA) as previously described (Goff et al., 2004). The comparative cycle threshold C_t method ($\Delta\Delta C_t$ method) was used for data analysis. Data from the control group was set as 1 or 100% and normalized relative quantities were shown. The same cDNA used for the microarrays was used to test the expression of GAP-43 and CRP1 in the NMLF after SCI. To study the expression of CRP1 in spinal cord caudal to the lesion site, total RNA was prepared from 4 millimeter pieces of spinal cord directly caudal to the lesion site. The primers used are as follows: zebrafish CRP1 (forward: 5'-TGCTTCCTGTGCATGGTTTG-3' and reverse: 5'-GGCCACCGTGGTACTGTCA-3'); zebrafish GAP-43 (forward: 5'-TCAGGAGATCAAGCAGGATGG-3' and reverse: 5'-GCCTTGTGAGCGTTTTCCTC-3'); zebrafish ribosomal protein P0 (forward: 5'-TCGGCTACCCAACTCTTGCT-3' and reverse: 5'-TGTTTCGACAGTGACAGCCAG-3'); rat CRP1 (forward: 5'-ACCACCAACCCCAATGCAT-3' and reverse: 5'-AGAAGATCGGCGGCTCTGAG -3') and rat GAPDH (forward: 5' -TCCTGCACCACCAACTGCTTAGCC-3' and reverse: 5'-GCCAAGGTCATCCATGAGCTGAAC-3').

In situ hybridization. Digoxigenin (DIG) labeled RNA sense and anti-sense probes for zebrafish CRP1 (NM_205567, 125bp - 554bp of coding sequence) and mouse CRP1 (NM_007791, full length) were generated using the Megascript^{TM} system (Ambion) according to the manufacturer's protocol and *in situ* hybridization was performed as

previously described (Becker et al., 1998; Lieberoth et al., 2003). Briefly, 20 μm-thick coronal sections containing NMLF were incubated with 0.1 N HCl for 10 minutes, followed by three washes in phosphate buffered saline (PBS), pH 7.4, and then digested for 10 minutes with 10 μg/ml proteinase-K (Roche, Indianapolis, IN) at room temperature, followed by fixation in 4% paraformaldehyde after 2 washes with glycine (2 mg/ml) in PBS, pH 7.4. Next, the sections were acetylated, dehydrated, air-dried, prehybridized, and subsequently hybridized with DIG-labeled probe at 55°C overnight. The hybridized probes were detected using alkaline phosphatase-coupled anti-DIG antibody (Roche) and color developed with nitro-blue tetrazolium and 5-bromo-4-chloro-3-indolyl phosphate (Roche). The same development time was used for sections from control and SCI animals. The neurons in NMLF can be easily identified by their anatomical location according to the atlas of zebrafish brain (Wullimann, 1996) and their large size (13-23 μm in diameter) (Becker et al., 1997), which is distinguished from the small size of glial cells (Becker et al., 1998). For profile counting, positively stained neurons in the NMLF from each animal (approximately 30 sections per animal) were counted with the experimenter blinded to the treatment of each fish.

Application of morpholinos and biocytin. Anti-sense morpholino (MO) oligonucleotides for zebrafish CRP1 (NM_205567) (5'-GTTTCCACCCCCAAGAGGCATCCTG-3') tagged with carboxyfluorescein at the 3' end, were designed and synthesized by Gene Tools company (Philomath, OR). Sequence for the standard control morpholino, which was also tagged with carboxyfluorescein at the 3' end, was 5'-CCTCTTACCTCAGTTACAATTTATA-3'. The MOs were dissolved in Danieau

solution (58 mM NaCl, 0.7 mM KCl, 0.4 mM $MgSO_4$, 0.6 mM $Ca(NO_3)_2$, 5 mM HEPES, pH 7.6) and applied as previously described (Becker et al., 1997; Becker et al., 2004). Gelfoam (Upjohn, Kalamazoo, MI) absorbed with 600 ng carboxyfluorescein-tagged MO (approximately 0.27 μl) for CRP1 or standard control was inserted into the spinal lesion site immediately after the transection. The MO is taken up by lesioned axons and retrogradely transported to the cells of origin in the brain, where protein synthesis for the target gene is blocked. The MO-treated fish were allowed to survive for 6 weeks.

Six weeks after the MO application, Gelfoam absorbed with the neuronal tracer biocytin (Sigma, saturated solution, approximately 0.27 μl) was applied to a secondary lesion site, which was 8 mm caudal to the brainstem-spinal cord junction, i.e. 4 mm caudal to the first spinal lesion site for MO application. Twenty-four hours later, the brains were dissected, embedded in OCT medium, and transversely frozen-sectioned. The biocytin was detected by the Vectastain ABC-DAB kit (Vector Laboratories, Burlingame, CA) as previously described (Becker et al., 1997). For profile counting, positively stained neurons in the NMLF of each animal (approximately 30 sections) were counted with the experimenter blinded to the treatment of each fish.

Locomotor analysis. Six weeks after the SCI and MO treatment (before the application of biocytin), the total distance moved by the MO-treated fish was measured to examine the locomotor recovery, and the tracking of freely moving fish was performed as previously described (Becker et al., 2004). Each fish was placed in a glass tank (50×30 cm) and allowed to move freely for 5 minutes while a video of each fish was taken using a camera

mounted above the tank. Swim paths were tracked and calculated with ANY-maze video tracking system (Stoelting Co, Wood Dale, IL).

Neuronal culture and transfection. Primary hippocampal neurons were prepared as described (Crozier et al., 2008). Hippocampi from E18 rat embryos were digested with 0.25% trypsin-EDTA for 10 minutes at 37°C, followed by trituration with a fire-polished Pasteur pipette in the plating medium (Neurobasal with 10% fetal bovine serum, Invitrogen, Carlsbad, CA). Neurons were plated onto coverslips coated with poly-D-lysine (100 μg/ml) (Sigma) and laminin (10 μg/ml) (Invitrogen). For some experiments (Figure 3), in order to show the morphology of growth cones, neurons were plated onto coverslips coated only with poly-D-lysine. Four hours after plating, medium was changed to Neurobasal with 2% B27 (Invitrogen). Dissociated neurons were transfected by electroporation using the Amaxa Nucleofector device (Lonza, Basel, Switzerland) immediately after dissociation. In some experiments, plasmids were cotransfected with pCAGdsRED at a ratio of 3:1. Neuronal morphology of transfected neurons was analyzed 48-72 h after plating.

The KCl treatment was performed as previously described (Redmond et al., 2002). At 3 days *in vitro* (DIV), neurons were stimulated with 50 mM KCl for the indicated times. Inhibitors APV (200 μM, Sigma), nifedipine (20 μM, Calbiochem, Gibbstown, NJ), KN62 (10 μM, Sigma), U0126 (25 μM, Sigma), KT5720 (5 μM, Sigma) and EGTA (2 mM, Sigma) were added 30 min before the addition of KCl (Redmond et al., 2002).

For the transfection necessary for KCl treatment or CaMKIV overexpression, hippocampal neurons were transfected at 2 DIV using Effectene (Qiagen). Transfected

neurons were treated with 50 mM KCl at 3 DIV and fixed at 5 DIV. Cotransfection of CaMKIV and shCRP1 or control shRNA was done with a ratio of 2:1 and neurons were fixed and analyzed at 5 DIV. N2a cells were cultured in DMEM with 1 mM sodium pyruvate and 10% fetal bovine serum (Invitrogen). N2a cells were transfected with Fugene 6 (Roche) according to the manufacturer's instructions.

DNA constructs. Mouse CRP1 was subcloned into pEGFP-N1 vector (Clontech, Mountain View, CA) using Nhe I and BamH I. Wild type (full length) CRP1, residues 1-79 of CRP1, and residues 1-65 of CRP1 were described before (Jang and Greenwood, 2009). CaMKIV-313 (constitutively active) and CaMKII-290 (constitutively active) were gifts from Dr. Richard Maurer (Oregon Health Sciences University, Portland, OR). CaMKIV-200A (dominant-negative) was a gift from Dr. Anthony R. Means (Duke University Medical Center, Durham, NC). KCREB (dominant-negative for CREB) was a gift from Dr. Michael E. Greenberg (Harvard Medical School, Boston, MA).

pSUPER-GFP (Oligoengine, Seattle, WA) was used to make shRNA. The siRNA sequence used for CRP1 (5'–GGGAAGTCCTGGCATAAGT-3') and the nonsense sequence used as negative control (5'-GCGCGCTATGTAGGATTCG-3') were subcloned into pSUPER-GFP vector according to the manufacturer's instructions.

Immunostaining**.** For immunostaining**,** neurons were fixed in freshly prepared 4% paraformaldehyde in 0.1 M phosphate buffer (pH 7.4) for 20 min. The cells were blocked and permeabilized with 3% donkey serum, 1% bovine serum albumin (BSA) and 0.2% Triton X-100 in PBS, which was followed by incubation with anti-CRP1 antibody (Santa

Cruz Biotechnology, Santa Cruz, CA, 1:200) and/or anti-β-tubulin III (Covance, Philadelphia, PA, 1:500) at 4°C overnight. Cells were then incubated for 2 hours with the secondary antibody (Alexa Fuor 488-conjugated anti-goat antibody, Molecular Probes, 1:800) diluted in PBS containing 1% BSA and 0.2% Triton X-100. For double staining of CRP1 and β-tubulin III, the cells were then incubated with Cy5-conjugated anti-mouse IgG (Molecular Probes, 1:800) after 3 washes. For the negative control, the primary antibody was replaced with normal goat IgG (Sigma). Phalloidin coupled to Texas Red (Invitrogen) was used to label actin filaments.

Western blot analysis. Goat anti-CRP1 (Santa Cruz, 1:500 or R&D systems, Minneapolis, MN, 1:400) or mouse anti-GAPDH (Millipore, Billerica, MA, 1:1000) were used as primary antibodies. HRP-conjugated donkey anti-goat (Promega, Madison, WI, 1:5000) or HRP-conjugated goat anti-mouse (Millipore, 1:5000) were used as secondary antibodies. The ECL detection system (Pierce, Rockford, IL) was used for signal detection. Quantitative analysis was performed using Kodak molecular imaging software version 4.0 (Carestream Molecular Imaging, New Haven, CT).

Image analysis. Images of transfected neurons were captured using a digital CCD camera attached to the side part of an inverted microscope driven by AxioVision software (Zeiss). Transfection experiments were carried out in duplicate wells and all experiments were repeated at least three times. Approximately 20 neurons per group were obtained each time. Captured neurons were traced and analyzed using Image J and Scion Image software as previously described (Dityatev et al., 2000). Since hippocampal neurons have

not developed dendritic spines at 3-5 DIV, so all long thin structures emerging from neurites shorter than 10 μm were counted as filopodia and others (longer than 10 μm) were counted as branch tips as previously described (Li et al., 2008). The longest neurite was recognized as an axon as described in Garvalov et al. (2007). Data are shown as mean values ± SEM and analyzed with Student's *t*-test with the level of significance set at $P < 0.05$.

Results

CRP1 is upregulated in the NMLF neurons after spinal cord injury (SCI) in zebrafish

To screen for novel growth associated genes that are involved in a successful regeneration response, microarrays were used to compare gene expression profiles after SCI. It has been reported that different nuclei with the capacity to regenerate their axons have similar expression patterns for growth associated genes, suggesting a shared molecular mechanism (Becker et al., 1998). The NMLF neurons mount a robust regeneration response after SCI (Becker et al., 1997; Becker et al., 1998; Becker et al., 2004). In addition, the NMLF is anatomically well defined, making it an excellent candidate to perform such a screening assay. Laser capture microdissection was used to isolate the NMLF from the brainstem sections of control and lesioned animals (Fig. 1A,B). The time point of 11 days post-injury was chosen for harvesting the NMLF because this is when neurons increase expression of growth associated genes and exhibit active axonal growth after SCI (Becker et al., 1998; Becker et al., 2004). Each condition (control or SCI) consisted of three microarrays, with the total RNA sample for each microarray prepared from laser-dissected NMLF tissues pooled from 3 animals and then amplified. GAP-43 is a well-known marker of axonal growth (Skene, 1989) and is upregulated in NMLF neurons and other nuclei capable of regeneration after SCI (Becker et al., 1998). Here, GAP-43 is used as a positive control for genes that are upregulated after SCI. The microarray data showed that the fold induction for GAP-43 mRNA after SCI was 1.121 (P = 0.014) compared to the sham-lesioned controls, while the fold induction for CRP1 mRNA was 1.145 (P = 0.003) (Fig. 1C), which is comparable to that

of GAP-43. The small upregulation of GAP-43 mRNA in this microarray data might be due to the limited numbers of NMLF neurons (about 60) in each brain. The microarray data for GAP-43 and CRP1 was confirmed by quantitative real-time PCR (qPCR), which showed the fold induction values were 3.45 and 1.44, respectively (Fig. 1D). The discrepancy in the fold inductions between microarray and qPCR might be due to the difference in the amplification methods and detection techniques used in those assays.

The upregulation of CRP1 mRNA after SCI in NMLF neurons was further validated by *in situ* hybridization. The NMLF neurons can be easily identified by their typical location and large size (13-23 μm in diameter) (Fig. 1E,F) (Wullimann, 1996; Becker et al., 1997), distinguishing them from glial cells, which are characterized by their small size (Becker et al., 1998). Signal for CRP1 mRNA was only observed in neurons in the NMLF. The number of CRP1 mRNA positive neurons was strongly increased in the NMLF at 11 days after SCI (Fig. 1E-G), indicating CRP1 may be a critical component of the neuron-intrinsic regeneration response.

In addition to regenerating neurons in the brain, the spinal cord caudal to the lesion site into which the regenerating axons regrow, also contributes to regeneration (Becker et al., 1998). The expression of CRP1 mRNA in the spinal cord region caudal to the lesion site was therefore also examined using qPCR. Unlike the response found in the NMLF, the expression of CRP1 mRNA caudal to the lesion site was slightly decreased at 11 days after SCI (Fig. 1H). This suggests that increased CRP1 mRNA expression is mainly associated with the intrinsic regenerative response of supraspinal neurons, and is not involved in the extrinsic response that creates a permissive environment for axonal regrowth.

CRP1 is essential for spinal cord regeneration in zebrafish

Anti-sense morpholino (MO) oligonucleotides have been used effectively to investigate the role of specific genes in zebrafish spinal cord regeneration (Becker et al., 2004). Like conventional neuronal tracers, MO can be absorbed by the injured axons at the lesion site and retrogradely transported into neuronal somata where the protein translation of the target gene is blocked. In the zebrafish SCI model, this can be accomplished by placing MO soaked Gelfoam into the spinal cord transection site. The inhibitory effect of MO can last for at least 6 weeks (the longest time point tested) (Becker et al., 2004). Gelfoam only or the standard control morpholino did not show any effect on neuronal viability or spinal cord regeneration (Becker et al., 2004).

The role of a gene in zebrafish spinal cord regeneration has been evaluated by two decisive parameters: locomotor recovery and axonal regrowth (Becker et al., 2004). The total distance moved by fish in 5 minutes is used to measure locomotor activity. The locomotor activity is reduced to approximately 5% of that in unlesioned fish at 1 week after SCI and generally recovers to 60% at 6 weeks. No additional improvement is observed after this point (Becker et al., 2004). The identification of neurons that have regenerated their axons beyond the lesion site is performed by applying the retrograde tracer biocytin 4 mm caudal to the transection site six weeks after the lesion. The degree of locomotor recovery and the number of retrogradely labeled neurons reflect the extent of spinal cord regeneration and these two parameters are usually correlated (Becker et al., 2004).

The role of CRP1 in spinal cord regeneration was investigated using MO specific for CRP1. Six weeks after SCI, fish treated with CRP1 MO showed a decrease in the total distance moved (312 ± 158 cm/5 min) compared with fish treated with control MO (1374 ± 365 cm/5 min) (Fig. 2D), indicating that CRP1 MO specifically impaired locomotor recovery. After locomotor analysis, the same fish were used to retrogradely label neurons which had regrown their axons 4 mm beyond the lesion site. In animals treated with CRP1 MO, the number of retrogradely labeled neurons was reduced (9.5 ± 2.8) compared to fish treated with control MO (30.5 ± 3.8) (Fig. 2A-C), suggesting CRP1 MO inhibits axonal regrowth after SCI. In agreement with previous findings (Becker et al., 2004), the fluorescein tag signal on the MOs was still detectable in the NMLF neurons 6 weeks after application. No difference was found in the number of cells having the fluorescein signal between control and experimental animals (data not shown), indicating that neurons survived the CRP1 and control MO applications equally well. Since antibodies to zebrafish CRP1 are not available, it was impossible to test how much the CRP1 MO reduced CRP1 protein expression. The combined observations show a positive correlation between reduced locomotor recovery and number of retrogradely labeled NMLF neurons in animals treated with CRP1 MO and indicate that CRP1 is required for successful spinal cord regeneration in zebrafish.

CRP1 colocalizes with actin in filopodia of growth cones in rat hippocampal neurons

Since little is known about the expression and function of CRP1 in the fish or mammalian nervous system, the expression of CRP1 was first investigated in the mouse CNS using

Western blot analysis. Expression of CRP1 protein was detected in all brain regions studied, including olfactory bulb, cortex, hippocampus, striatum, thalamus, cerebellum, brain stem and spinal cord (see supplemental data). *In situ* hybridization confirmed the widespread expression of CRP1 and showed that neurons in the cerebral cortex and hippocampus, and cerebellar Purkinje cells were positive for CRP1 mRNA (see supplemental data), which is consistent with a previous report (McLaughlin et al., 1994). To identify the cell types expressing CRP1 protein, we used immunohistochemistry but were not able to detect a significant signal for CRP1. This may be due to the low expression level of CRP1 protein or the inability of our antibody to detect CRP1 when used for immunohistochemistry.

In light of this result, we tried to detect expression of CRP1 protein in cultured rat hippocampal neurons by immunostaining. Detectable CRP1 signal was seen as early as one day *in vitro* (DIV). When neurons were cultured on coverslips coated with poly-D-lysine and laminin, accumulation of CRP1 was observed at the tips of neurites (see supplemental data). In neurons cultured on coverslips coated only with poly-D-lysine, CRP1 was observed in the growth cones and colocalized with actin filaments in filopodia (Fig. 3A-G). The location of CRP1 in filopodia, which are composed of bundled actin, is consistent with a report showing that CRP1 acts as an actin-bundling protein (Tran et al., 2005). The distribution of CRP1 in neurons at 3 DIV was similar to that of neurons at 1 DIV (Fig. 3K,L). However, the expression pattern of CRP1 was different in β-tubulin III negative non-neuronal cells. Although a weak signal for CRP1 was observed in the cell body of these cells, no colocalization of CRP1 and actin filaments was detected (Fig. 3H-

J). Thus, the different expression pattern of CRP1 observed in neuronal and non-neuronal cells suggests specific functions for CRP1 in the neuronal growth cone.

CRP1 is required for dendritic growth

To investigate the functional role of CRP1, RNA interference (RNAi) was used to reduce the expression of CRP1 in cultured rat hippocampal neurons. A short hairpin RNAi sequence against both mouse and rat CRP1 was designed and incorporated into the pSUPER-GFP vector (Chen and Firestein, 2007). The negative control shRNA with no potential mRNA target did not show any toxic effects when used in cultured neurons as previously reported (Li et al., 2008). The vector expressing CRP1 shRNA (shCRP1) not only reduced CRP1 mRNA levels (Fig. 4A), but also decreased protein expression levels in N2A cells when compared to control shRNA (Fig. 4B). Hippocampal neurons were transfected with either CRP1 shRNA or control shRNA (CON) immediately after dissociation and neuronal morphology was analyzed 2 days later. Neither shRNA affected cell viability (data not shown). The number of primary neurites in neurons transfected with shCRP1 was decreased compared to neurons transfected with the negative control shRNA (Fig. 4C-E). Knock-down of CRP1 also reduced the number of neuritic branches (Fig. 4F) and filopodia (Fig. 4G). Moreover, neurons transfected with shCRP1 were reduced in total length of neurites compared to neurons transfected with control shRNA (Fig. 4H). However, shCRP1 did not affect axonal length (Fig. 4I), suggesting that CRP1 is involved in dendritic rather than axonal growth (Fig. 4J) in rat hippocampal neurons.

The function of CRP1 in neurons was further investigated in gain-of-function experiments. Neuronal morphology was examined at 3 DIV after the dissociated neurons were transfected with GFP-CRP1 or control GFP vectors (Fig. 5A-F). Overexpression of CRP1 in hippocampal neurons increased the number of neuritic branches (Fig. 5G) and filopodia (Fig. 5H), but not the number of primary neurites (data not shown). Also, overexpression of CRP1 did not show increases in the total length of neurites or dendrites (data not shown). Since knock-down of CRP1 decreased the number of primary neurites and neurite length, this suggests that CRP1 functions as a necessary, but not sufficient, component for neurite remodeling. The role for CRP1 in filopodia formation was further investigated in COS-7 cells by cotransfection with Cdc42, a well-known small GTPase involved in filopodia formation and neurite outgrowth in neurons. When CRP1 was co-overexpressed with a constitutively active form of Cdc42, the percentage of cells with filopodia was increased (see supplemental data), suggesting a possible regulatory effect of Cdc42 on CRP1.

It has been reported that CRP1 can directly bundle actin filaments and its LIM1 and GR1 (glycine repeat 1) domains are necessary for this ability (Jang and Greenwood, 2009). Since overexpression of CRP1 in neurons increased the number of neuritic branches and filopodia, we next studied whether this effect is mediated by its actin-bundling activity by using different segments of CRP1 with different actin-bundling ability. While residues 1-79 of CRP1, which contain the LIM1 and GR1 domains (Fig. 5I), retain its actin-bundling ability, residues 1-69, which only contain the LIM1 domain (Fig. 5I), lose this function (Jang and Greenwood, 2009). Overexpression of residues 1-79 increased the number of neuritic branches (Fig. 5J) and filopodia (Fig. 5K) as well as

the wild type CRP1, while overexpression of residues 1-69 did not show this effect (Fig. 5J,K). Thus, the effect of CRP1 in regulating neuritic branching and filopodia formation is mediated, at least partly, by its actin-bundling activity.

CRP1 is upregulated by Ca^{2+} influx following depolarization and is required for Ca^{2+}-dependent dendritic growth

Neuronal activity influences many aspects of neuron function, such as dendritic arborization (reviewed in Redmond, 2008). In smooth muscle cells, CRP1 expression is increased following depolarization induced by high K^+ (Najwer and Lilly, 2005), suggesting that CRP1 mediates the consequences of depolarization. To determine whether CRP1 is involved in neuronal activity-dependent dendritic growth, CRP1 expression was examined in neurons after depolarization. Neurons were treated with 50 mM KCl at 3 DIV as previously described (Redmond et al., 2002) and CRP1 mRNA levels were studied at different time points after addition of KCl. Six hours after the addition of KCl, CRP1 mRNA expression was slightly decreased but was then upregulated from 12 hours onward (Fig. 6A) continuing up to 48 hours after KCl addition. Not only CRP1 mRNA levels, but also CRP1 protein levels were increased when tested 48 hours after addition of KCl (Fig. 6B,C).

To investigate whether Ca^{2+} influx is required for the upregulation of CRP1 induced by KCl stimulation, neurons were treated with 2 mM EGTA, an extracellular Ca^{2+} chelator, with or without KCl. EGTA alone showed inhibition on CRP1 mRNA expression after 24 hours (Fig. 6D), indicating that Ca^{2+} influences CRP1 expression under basal activity conditions. When cells were treated with KCl in the presence of

EGTA, upregulation of CRP1 mRNA levels were completely blocked (Fig. 6D). This observation suggests that Ca^{2+} mediates the KCl-mediated influence on CRP1 mRNA expression. In neurons, two primary Ca^{2+} channels, namely NMDA receptors and voltage-sensitive Ca^{2+} channels (L-VSCCs), mediate Ca^{2+} influx (Ghosh and Greenberg, 1995; Redmond et al., 2002). To address which type of Ca^{2+} channel is responsible for the Ca^{2+}-dependent upregulation of CRP1 mRNA, the inhibitors APV (for NMDA receptors) and nifedipine (for L-VSCCs) were tested. In the presence of KCl, both inhibitors partially inhibited upregulation of CRP1 mRNA levels (Fig. 6E). Although nifedipine showed a more inhibitory effect than APV, it did not completely block the upregulation of CRP1 mRNA levels (Fig. 6E). Upregulation of CRP1 mRNA was completely blocked when both APV and nifedipine were used together (Fig. 6E), indicating that both NMDA receptors and L-VSCCs are required.

Since Ca^{2+} regulates KCl-induced dendritic growth (reviewed in Redmond, 2008), we tested whether CRP1 is involved in Ca^{2+}-dependent dendritic growth. Hippocampal neurons were therefore transfected with control shRNA or shCRP1 at 2 DIV and treated with KCl at 3 DIV. Neuronal morphology was examined at 5 DIV. ShCRP1 reduced total dendritic length and total number of dendritic tips when compared with control shRNA (Fig. 6F,H,J,K). Consistent with the results obtained by other groups (Redmond et al., 2002; Yu and Malenka, 2003; Wayman et al., 2006; Tai et al., 2008), KCl treatment increased both the total dendritic length and total number of dendritic tips in neurons transfected with control shRNA (Fig. 6G,I,J,K). However, knock-down of CRP1 expression with shCRP1 significantly inhibited the dendritic growth induced by KCl (Fig. 6J,K), suggesting that CRP1 is required for the influence of Ca^{2+} on dendritic growth.

The inhibitory effect of shCRP1 on Ca^{2+}-dependent dendritic growth was not complete, suggesting that other signaling molecules than CRP1 are involved.

CaMKIV and CREB mediate the Ca^{2+}-induced upregulation of CRP1 expression

To analyze biochemical mechanisms underlying the Ca^{2+}-induced upregulation of CRP1 expression, three primary signaling intermediates for the Ca^{2+} signaling pathway in neurons were studied: Ca^{2+}/calmodulin-dependent protein kinases (CaMKI, II and IV), mitogen-activated protein kinases (MAPK), and protein kinase A (PKA) (Ghosh and Greenberg, 1995; Redmond et al., 2002). An inhibitor of MAPK (U0126) did not affect CRP1 mRNA levels when used alone or together with KCl in comparison with the control groups (Fig. 7B). However, KN62, an inhibitor of all CaM kinases, completely blocked the upregulation of CRP1 mRNA induced by KCl stimulation (Fig. 7A). Inhibiting PKA activation (KT5720), on the other hand, increased CRP1 mRNA expression (Fig. 7C). Taken together, these data indicate that the effect of Ca^{2+} influx on CRP1 expression is the net result of several converging pathways, similar to those on dendritic growth (Redmond et al., 2002).

Of the three kinds of CaM kinases involved in functions in neurons, CaMKI, II, and IV, only the roles of CaMKII and CaMKIV were analyzed, since the MAPK pathway, which mediates the effect of CaMKI (Wayman et al., 2006), did not affect CRP1 expression. Constitutively active forms of CaMKII and CaMKIV were used as previously described (Sun et al., 1994). Considering the limitations regarding transfection of cultured primary neurons, such as the age of cultured neurons (only freshly dissociated neurons can be used with nucleofector), the efficiency of transfection and protein

expression, the time window for upregulation of CRP1 induced by overexpression of active forms of CaMKII or CaMKIV, we resorted to the neuroblastoma cell line N2a for this experiment. Similar to what was observed in primary culture of neurons, KCl stimulation also induced upregulation of CRP1 mRNA levels in N2a cells (Fig. 7D). The constitutively active CaMKIV (caCaMKIV), but not caCaMKII, increased CRP1 mRNA expression (Fig. 7D). The role of CaMKIV was confirmed by using a dominant-negative form of CaMKIV (dnCaMKIV) (Lemrow et al., 2004), which blocked the upregulation of CRP1 mRNA levels induced by KCl (Fig. 7E).

Since CREB is the best-characterized transcription factor target of CaMKIV (Redmond et al., 2002; Redmond, 2008; Tai et al., 2008), we investigated whether CREB mediates upregulation of CRP1 using a dominant-negative mutant of CREB (KCREB) (Walton et al., 1992). As shown in Fig. 7F, CaMKIV-induced upregulation of CRP1 was suppressed by KCREB expression. Similarly, KCREB also blocked the stimulation of CRP1 by KCl (Fig. 7F). These results demonstrate the requirement for CaMKIV and CREB activity in Ca^{2+}-induced upregulation of CRP1 expression.

It has been reported that constitutively active CaMKIV alone is sufficient to increase dendritic growth (Redmond et al., 2002; Yu and Malenka, 2003; Tai et al., 2008). Since caCaMKIV increased CRP1expression in neurons, we studied whether CRP1 contributes to CaMKIV-induced dendritic growth using shCRP1. Consistent with previous work (Redmond et al., 2002; Yu and Malenka, 2003; Tai et al., 2008), overexpression of caCaMKIV indeed increased dendritic growth as measured by dendritic length and total number of dendritic tips (Fig.7 G,H,K,L). Knock-down of CRP1 expression significantly inhibited the dendritic growth induced by caCaMKIV (Fig. 7G-L). Taken together, these

results support the view that CRP1 is required for Ca^{2+}-dependent dendritic growth of hippocampal neurons.

Discussion

Our study presents evidence for the requirement of CRP1 in spinal cord regeneration in zebrafish. Using laser capture microdissection and microarray analysis, we found that CRP1 is upregulated in the NMLF neurons during spinal cord regeneration. *In vivo* knock-down of CRP1 expression with a specific MO impaired locomotor recovery and axon regeneration, indicating that CRP1 upregulation is an essential part of the natural regeneration mechanism in spinal cord injured adult zebrafish. Successful spinal cord regeneration requires at least two critical factors: the ability of an injured neuron to regrow its axon and a supportive extracellular environment for axon regeneration (Bulsara et al., 2002). In addition, rearrangements of intraspinal connections of interneurons involving pre- and post-synaptic structures need to be considered. Interestingly, CRP1 mRNA levels are only upregulated in the cell bodies of regenerating neurons (NMLF neurons in the brainstem), but not in the caudal part of spinal cord, into which the severed axons re-grow. This suggests that CRP1 is only associated with the neuron-intrinsic regeneration response and is not involved in the extrinsic response that creates a permissive environment for axon regeneration. Thus, we propose that the effect of CRP1 MO on axon regrowth is mainly due to the loss of CRP1 expression in those neurons that regrow their severed axons.

The amino acid sequence of CRP1 is very similar among vertebrates with more than 80% identity between human, mouse, rat, chicken, quail and zebrafish, suggesting its conserved function (McLaughlin et al., 1994). Because of this extensive sequence conservation and the inability to culture zebrafish NFLM neurons, we used cultured mammalian neurons to further elucidate the function of CRP1 in the nervous system. In

cultured primary rat neurons, endogenous CRP1 accumulates in the growth cone and is enriched in filopodia, which indicates that it likely functions in the growth cone of the regenerating axons in zebrafish. Filopodia are finger-like structures composed of tightly oriented parallel actin bundles that extend radially from the lamellipodial actin meshwork at the growth cone tip, thus playing a critical role in neurite outgrowth (Mattila and Lappalainen, 2008). The location of CRP1 in filopodia is consistent with the previous demonstration that CRP1 directly interacts with actin filaments and functions as an actin bundling protein (Tran et al., 2005; Jang and Greenwood, 2009). Moreover, the expression pattern of CRP1 is similar to that of fascin, another actin-bundling protein in that it is localized along the entire length of filopodia (Cohan et al., 2001; Vignjevic et al., 2006), suggesting that CRP1 serves an important role in filopodia formation via its actin-bundling activity. Consistent with this idea, our loss-of-function and gain-of-function experiments provide evidence for this essential role of CRP1 in filopodia formation. Filopodia exert their functions in neurite outgrowth by sensing conducive molecules in the environment resulting in subsequent downstream signaling, which is required for neurite extension (Mattila and Lappalainen, 2008). Depletion of proteins involved in filopodia formation therefore not only inhibits filopodia formation but also impairs neuritogenesis (Dent et al., 2007; Kwiatkowski et al., 2007; Korobova and Svitkina, 2008). Filopodia formation is among the first structural changes to occur at the regenerating axon tip and is required for growth cone formation after injury (Welnhofer et al., 1997). Combining the role for CRP1 in filopodia formation, we propose that CRP1 is necessary for spinal cord regeneration because of its role for the normal function of growth cones.

Since CRP1 MO inhibits axon regeneration in zebrafish, it was not surprising that shCRP1 inhibited neurite outgrowth in cultured rat hippocampal neurons *in vitro*. However, under these conditions neurons transfected with shCRP1 elaborate axons with normal length. The discrepancy between our observations of CRP1 on axon regrowth in the injured spinal cord of zebrafish, on the one hand, and dendritic neurite extension in cultured hippocampal neurons, on the other hand, is likely due to differences in the type and age of neurons, animal species, and the more complex conditions in an animal versus those in the less complex environment of primary cultures of neurons. Since it is not possible to culture NMLF neurons from adult zebrafish *in vitro*, these questions will be difficult to resolve, particularly since the molecular mechanisms involved in axon growth during development versus regrowth after injury in the adult are largely unknown. Our data indicates that CRP1 affects axon regeneration in the injured zebrafish spinal cord because of its function in filopodia formation, being in agreement with the observation that without Ena/VASP proteins which are molecules essential for filopodia formation, cortical neurons fail to form filopodia, resulting in deficiencies in axon tract formation *in vivo* (Dent et al., 2007; Kwiatkowski et al., 2007). However, it is conceivable that even in the same species, different types of neurons use different mechanisms for filopodia formation and subsequent axon outgrowth or regrowth. For example, in Ena/VASP null mice, while cortical neurons can not elaborate axon tracts *in vivo*, neurons outside the cortex do form axons (Dent et al., 2007; Kwiatkowski et al., 2007). This effect may be due to differences in intrinsic and/or extrinsic factors that enable different types of neurons to form filopodia and subsequently extend an axon (Dent et al., 2007; Kwiatkowski et al., 2007). Also, in invertebrates, loss of Ena/VASP does not block

formation of axons (Krause et al., 2003). The combined observations suggest that both species-specific and neuronal subtype differences affect axon development and regeneration.

In vitro, the knock-down of endogenous CRP1 in cultured hippocampal neurons inhibited filopodia formation and dendritic growth. This effect is similar to that of other molecules, such as Ena/VASP (Lebrand et al., 2004; Dent et al., 2007), MARCKs (myristoylated, alanine-rich C kinase substrate) (Calabrese and Halpain, 2005; Li et al., 2008), TRPC6 (transient receptor potential channel 6) (Tai et al., 2008; Zhou et al., 2008), or septin 7 (Xie et al., 2007), all of which are important not only for filopodia or spine formation, but also for dendritic growth. Since filopodia are not only important for axonal growth, but also develop into dendritic spines (Yuste and Bonhoeffer, 2004; Mattila and Lappalainen, 2008), it is not surprising that proteins involved in filopodia formation are also involved in spine formation. Moreover, it has been demonstrated that many fine filopodial protrusions rapidly extend and retract on the dendritic shafts of hippocampal neurons during early dendritic development, directly transforming into nascent dendritic branches, which suggests that neurite branching is initiated by filopodia (Dailey and Smith, 1996; Lalli and Hall, 2005; Hall and Lalli, 2010). A number of studies showed that neuronal activity can regulate dendritic architecture and Ca^{2+} influx is a critical primary event in this response (reviewed in Redmond, 2008). Although it has been shown that Ca^{2+}-dependent dendritic growth requires CREB-mediated transcription, little is known about the target genes of Ca^{2+} that mediate dendritic growth. One potential target is brain-derived neurotrophic factor, which is upregulated by Ca^{2+} influx in primary neurons (Ghosh et al., 1994). Another secreted protein, Wnt-2, has been shown to be

upregulated in neurons after depolarization and it is involved in activity-induced dendritic growth (Wayman et al., 2006). Here, we found that CRP1 expression is not only upregulated by Ca^{2+} influx in neurons but also required for Ca^{2+}-dependent dendritic growth. Consistent with this, similar intracellular signaling molecules affected by Ca^{2+} influx are shared by CRP1 expression and dendritic growth (Redmond et al., 2002). Activation of PKA inhibits dendritic growth as well as the expression of CRP1, whereas CaMKIV mediates Ca^{2+}-dependent dendritic growth and increases CRP1 expression. Taken together, upregulation of CRP1 significantly contributes to Ca^{2+}-dependent dendritic growth not only during development but also in activity-induced remodeling of synaptic connections in the adult. Whether recognition molecules at the cell surface and/or in the extracellular matrix guide this formation of axonal and/or dendritic filopodia trigger the activities of CRP1 remains to be investigated. Preliminary results (data not shown) indicate that the neurite outgrowth promoting immunoglobulin superfamily molecules L1 and NCAM are not involved.

In conclusion, using zebrafish as a model to study the mechanisms underlying successful axon regrowth, we identified CRP1 as an essential molecule for spinal cord regeneration in the spontaneously regenerating adult zebrafish. In addition, we provide *in vitro* evidence for the important role played by CRP1 in filopodia formation and neurite remodeling, expanding on the current scanty knowledge regarding the functional role of CRP1 in the vertebrate central nervous system. Collectively, these data provide firm ground for future attempts to increase CRP1 expression in adult mammals for improved functional recovery after spinal cord injury, and other acute or possibly even chronic injuries of the adult mammalian central nervous system.

References

Becker CG, Becker T (2008) Adult zebrafish as a model for successful central nervous system regeneration. Restor Neurol Neurosci 26:71-80.

Becker CG, Lieberoth BC, Morellini F, Feldner J, Becker T, Schachner M (2004) L1.1 is involved in spinal cord regeneration in adult zebrafish. J Neurosci 24:7837-7842.

Becker T, Wullimann MF, Becker CG, Bernhardt RR, Schachner M (1997) Axonal regrowth after spinal cord transection in adult zebrafish. J Comp Neurol 377:577-595.

Becker T, Bernhardt RR, Reinhard E, Wullimann MF, Tongiorgi E, Schachner M (1998) Readiness of zebrafish brain neurons to regenerate a spinal axon correlates with differential expression of specific cell recognition molecules. J Neurosci 18:5789-5803.

Bulsara KR, Iskandar BJ, Villavicencio AT, Skene JH (2002) A new millenium for spinal cord regeneration: growth-associated genes. Spine (Phila Pa 1976) 27:1946-1949.

Chang DF, Belaguli NS, Iyer D, Roberts WB, Wu SP, Dong XR, Marx JG, Moore MS, Beckerle MC, Majesky MW, Schwartz RJ (2003) Cysteine-rich LIM-only proteins CRP1 and CRP2 are potent smooth muscle differentiation cofactors. Dev Cell 4:107-118.

Chen H, Firestein BL (2007) RhoA regulates dendrite branching in hippocampal neurons by decreasing cypin protein levels. J Neurosci 27:8378-8386.

Cohan CS, Welnhofer EA, Zhao L, Matsumura F, Yamashiro S (2001) Role of the actin bundling protein fascin in growth cone morphogenesis: localization in filopodia and lamellipodia. Cell Motil Cytoskeleton 48:109-120.

Crozier RA, Bi C, Han YR, Plummer MR (2008) BDNF modulation of NMDA receptors is activity dependent. J Neurophysiol 100:3264-3274.

Dent EW, Kwiatkowski AV, Mebane LM, Philippar U, Barzik M, Rubinson DA, Gupton S, Van Veen JE, Furman C, Zhang J, Alberts AS, Mori S, Gertler FB (2007) Filopodia are required for cortical neurite initiation. Nat Cell Biol 9:1347-1359.

Dityatev A, Dityateva G, Schachner M (2000) Synaptic strength as a function of post- versus presynaptic expression of the neural cell adhesion molecule NCAM. Neuron 26:207-217.

Ghosh A, Greenberg ME (1995) Distinct roles for bFGF and NT-3 in the regulation of cortical neurogenesis. Neuron 15:89-103.

Goff LA, Bowers J, Schwalm J, Howerton K, Getts RC, Hart RP (2004) Evaluation of sense-strand mRNA amplification by comparative quantitative PCR. BMC Genomics 5:76-84.

Irizarry RA, Hobbs B, Collin F, Beazer-Barclay YD, Antonellis KJ, Scherf U, Speed TP (2003) Exploration, normalization, and summaries of high density oligonucleotide array probe level data. Biostatistics 4:249-264.

Jain MK, Kashiki S, Hsieh CM, Layne MD, Yet SF, Sibinga NE, Chin MT, Feinberg MW, Woo I, Maas RL, Haber E, Lee ME (1998) Embryonic expression suggests an important role for CRP2/SmLIM in the developing cardiovascular system. Circ Res 83:980-985.

Jang HS, Greenwood JA (2009) Glycine-rich region regulates cysteine-rich protein 1 binding to actin cytoskeleton. Biochem Biophys Res Commun 380:484-488.

Korobova F, Svitkina T (2008) Arp2/3 complex is important for filopodia formation, growth cone motility, and neuritogenesis in neuronal cells. Mol Biol Cell 19:1561-1574.

Krause M, Dent EW, Bear JE, Loureiro JJ, Gertler FB (2003) Ena/VASP proteins: regulators of the actin cytoskeleton and cell migration. Annu Rev Cell Dev Biol 19:541-564.

Kwiatkowski AV, Rubinson DA, Dent EW, Edward van Veen J, Leslie JD, Zhang J, Mebane LM, Philippar U, Pinheiro EM, Burds AA, Bronson RT, Mori S, Fassler R, Gertler FB (2007) Ena/VASP Is Required for neuritogenesis in the developing cortex. Neuron 56:441-455.

Latonen L, Jarvinen PM, Laiho M (2008) Cytoskeleton-interacting LIM-domain protein CRP1 suppresses cell proliferation and protects from stress-induced cell death. Exp Cell Res 314:738-747.

Lemrow SM, Anderson KA, Joseph JD, Ribar TJ, Noeldner PK, Means AR (2004) Catalytic activity is required for calcium/calmodulin-dependent protein kinase IV to enter the nucleus. J Biol Chem 279:11664-11671.

Li H, Chen G, Zhou B, Duan S (2008) Actin filament assembly by myristoylated alanine-rich C kinase substrate-phosphatidylinositol-4,5-diphosphate signaling is critical for dendrite branching. Mol Biol Cell 19:4804-4813.

Lilly B, Clark KA, Yoshigi M, Pronovost S, Wu ML, Periasamy M, Chi M, Paul RJ, Yet SF, Beckerle MC (2010) Loss of the serum response factor cofactor, cysteine-rich protein 1, attenuates neointima formation in the mouse. Arterioscler Thromb Vasc Biol 30:694-701.

Liss B, Haeckel O, Wildmann J, Miki T, Seino S, Roeper J (2005) K-ATP channels promote the differential degeneration of dopaminergic midbrain neurons. Nat Neurosci 8:1742-1751.

Mattila PK, Lappalainen P (2008) Filopodia: molecular architecture and cellular functions. Nat Rev Mol Cell Biol 9:446-454.

Najwer I, Lilly B (2005) Ca2+/calmodulin-dependent protein kinase IV activates cysteine-rich protein 1 through adjacent CRE and CArG elements. Am J Physiol Cell Physiol 289:C785-793.

Pomies P, Louis HA, Beckerle MC (1997) CRP1, a LIM domain protein implicated in muscle differentiation, interacts with alpha-actinin. J Cell Biol 139:157-168.

Redmond L (2008) Translating neuronal activity into dendrite elaboration: signaling to the nucleus. Neurosignals 16:194-208.

Redmond L, Kashani AH, Ghosh A (2002) Calcium regulation of dendritic growth via CaM kinase IV and CREB-mediated transcription. Neuron 34:999-1010.

Skene JH (1989) Axonal growth-associated proteins. Annu Rev Neurosci 12:127-156.

Sun P, Enslen H, Myung PS, Maurer RA (1994) Differential activation of CREB by Ca2+/calmodulin-dependent protein kinases type II and type IV involves phosphorylation of a site that negatively regulates activity. Genes Dev 8:2527-2539.

Tai Y, Feng S, Ge R, Du W, Zhang X, He Z, Wang Y (2008) TRPC6 channels promote dendritic growth via the CaMKIV-CREB pathway. J Cell Sci 121:2301-2307.

Tran TC, Singleton C, Fraley TS, Greenwood JA (2005) Cysteine-rich protein 1 (CRP1) regulates actin filament bundling. BMC Cell Biol 6:45-57.

Vignjevic D, Kojima S, Aratyn Y, Danciu O, Svitkina T, Borisy GG (2006) Role of fascin in filopodial protrusion. J Cell Biol 174:863-875.

Wayman GA, Impey S, Marks D, Saneyoshi T, Grant WF, Derkach V, Soderling TR (2006) Activity-dependent dendritic arborization mediated by CaM-kinase I activation and enhanced CREB-dependent transcription of Wnt-2. Neuron 50:897-909.

Welnhofer EA, Zhao L, Cohan CS (1997) Actin dynamics and organization during growth cone morphogenesis in Helisoma neurons. Cell Motil Cytoskeleton 37:54-71.

Wullimann MF, B. Rupp, and H. Reichert (1996) Neuroanatomy of the Zebrafish Brain: A Topological Atlas. Basel: Birkhauser.

Xie Y, Vessey JP, Konecna A, Dahm R, Macchi P, Kiebler MA (2007) The GTP-binding protein Septin 7 is critical for dendrite branching and dendritic-spine morphology. Curr Biol 17:1746-1751.

Yu X, Malenka RC (2003) Beta-catenin is critical for dendritic morphogenesis. Nat Neurosci 6:1169-1177.

Figure legends

Figure 1. CRP1 is upregulated in the NMLF neurons at 11 days after SCI in zebrafish. (**A**,**B**) NMLF were collected from coronal sections of the brainstem by using laser capture microdissection, then used for RNA preparation and microarray analysis. (**C**) Graph of normalized fold changes for GAP-43 (1.121 ± 0.015, $P < 0.05$) and CRP1 (1.145 ± 0.008, $P < 0.01$) from microarray analysis. (**D**) Quantitative real-time PCR (qPCR) shows that both GAP-43 and CRP1 are upregulated in the NMLF at 11 days after SCI. (**E-G**) *In situ* hybridization of the NMLF from fish with sham-lesion (referred to as CON, **E**) or SCI (**F**) shows that the number of CRP1 mRNA positive neurons (arrows) is increased approximately five-fold (**G**) at 11 days after SCI. (**H**) qPCR shows that CRP1 levels are downregulated in the caudal part of the spinal cord at 11 days after SCI. **A**-**D**, n = 3, **E**-**G**, n = 6, **H**, n = 3; * $P < 0.05$, *t*-test; Mean values ± SEM are shown. Scale bars: **A**, **B**, 1 mm; **E**, **F**, 50 μm.

Figure 2. CRP1 is essential for successful spinal cord regeneration. Immediately after SCI, morpholinos (MO) were applied to the lesion site. MO are taken up by injured axons and retrogradely transported to neuronal somata in the brainstem. The total distance moved and numbers of retrogradely labeled neurons in the NMLF (biocytin label) are measured 6 weeks after SCI and MO application. (**A**,**B**) MO for CRP1 (CRP1 MO, **B**) reduce biocytin-labeled neurons (arrowheads) in the NMLF when compared to control MO (CON MO, **A**). Biocytin was applied 4 mm caudal to the lesion site. (**C**) Quantification shows a three-fold decrease in numbers of biocytin-labeled neurons in fish received CRP1 MO compared to fish received CON MO. (**D**) Total distance moved by

fish treated with CRP1 MO is decreased compared to fish treated with CON MO. n = 6 (CON MO) and n = 8 (CRP1 MO); * $P < 0.05$, *t*-test; Mean values ± SEM are shown. Scale bar, 50 μm.

Figure 3. Endogenous CRP1 accumulates in filopodia of growth cones and colocalizes with actin in cultured rat hippocampal neurons. (**A**-**J**) Representative images of hippocampal neurons at 1 DIV incubated with CRP1 antibody (**A**,**E**,**H**), β-tubulin III antibody (**C**) and Texas-red phalloidin (for actin) (**B**,**F**,**I**). CRP1 is expressed in neurons that are β-tubulin III positive (**C**) and is weakly expressed in non-neuronal cells that are β-tubulin III negative (**C**). CRP1 accumulates in filopodia of growth cones and colocalizes with actin (**E**-**G**). No colocalization of CRP1 and actin is observed in non-neuronal cells (**H**-**J**). (**K**,**L**) Neurons at 3 DIV show colocalization of CRP1 and actin in growth cones. **E** through **G** are enlargements of boxed area 1 and **H** through **J** are enlargements of boxed area 2. Scale bars: **A**-**D**, **K**, **L**, 50 μm; **E**-**J**, 25 μm.

Figure 4. CRP1 is required for dendritic growth in hippocampal neurons. (**A**) Downregulation of CRP1 mRNA levels by shCRP1. N2a cells were transfected with pSUPER vector either encoding CRP1 shRNA (shCRP1) or control shRNA (CON). Levels of CRP1 mRNA were analyzed by qPCR two days after transfection. (**B**) Downregulation of CRP1 protein levels by shCRP1. N2a cells were transfected with shCRP1 or control shRNA (CON) and CRP1 protein levels were analyzed 48 hours later by Western blot. GAPDH served as loading control. (**C**,**D**) Knock-down of endogenous CRP1 inhibits dendritic growth of hippocampal neurons cotransfected with DsRed and

either shCRP1 or control shRNA (CON) at a ratio of 1:3. The morphology of neurons was analyzed by assessing DsRed expression 48 hours after transfection with nucleofector. Neurons transfected with shCRP1 (arrows in **D**) have less dendrites when compared to neurons transfected with control shRNA (arrow in **C**). Knock-down of CRP1 decreases the number of primary neurites (**E**), the number of neurite branches (**F**) and the number of filopodia (**G**). Inhibition effect of shCRP1 on total length of neurites (**H**) is mainly due to inhibition on dendritic length (**J**), but not axonal length (**I**). n = 3 (**A**,**B**) or n = 60 (**E**-**J**); * $P < 0.05$, *t*-test; Mean values ± SEM are shown. Scale bar, 50 μm.

Figure 5. Overexpression of CRP1 increases branches and filopodia on neurites, which requires its actin-bundling ability. (**A**-**F**) Overexpression of CRP1 increases the number of branches and filopodia on neurites. Neuronal morphology was analyzed 3 days after transfection with nulceofector. CRP1 transfected neurons (**D**) have more branches and filopodia along their neurites (**E**,**F**) when compared with GFP transfected neurons (**A**-**C**). **B** and **C** are enlargements of boxed areas 1 and 2, respectively. **E** and **F** are enlargements of boxed areas 3 and 4, respectively. (**G**,**H**) Quantification shows that overexpression of CRP1 increased the number of branches (**G**) and filopodia (**H**) on neurites. (**I**) Diagram of wild type (WT) CRP1 and truncated forms of CRP1 used in this study. While residues 1-79 of CRP1 retain its actin-bundling ability and localization to the actin cytoskeleton, residues 1-65 do not. (**J**,**K**) The actin-bundling ability of CRP1 is required for its effect on neurite branching (**J**) and filopodia formation (**K**) in neurons. n

= 60; * $P < 0.05$, *t*-test; Mean values ± SEM are shown. Scale bars: **A, D** 50 μm; **B**, **C**, **E**, **F**, 25 μm.

Figure 6. CRP1 expression is upregulated by Ca^{2+} influx in hippocampal neurons and is involved in Ca^{2+}-dependent dendritic growth. (**A**) Depolarization induced by 50 mM KCl increases CRP1 mRNA expression. CRP1 mRNA expression is slightly downregulated at 6 hours but is then upregulated from 12 hours, and this upregulation continues to 24 hours and 48 hours. (**B**,**C**) KCl stimulation increases CRP1 protein expression as analyzed by Western blot analysis 48 hours after addition of KCl. GAPDH served as loading control. (**D**) EGTA (2 mM) treatment inhibits CRP1 expression at basal level and blocks the upregulation effect of KCl on CRP1 mRNA levels. (**E**) Upregulation of CRP1 expression is completely blocked only when both inhibitors for L-VSCCs (NIF) and NMDA receptors (APV) were applied together. (**F-I**) Representative images of neurons transfected at 2 DIV with shCRP1 or control shRNA (CON) and treated with or without 50 mM KCl at 3 DIV for 48 hours. (**J**,**K**) Quantification of total dendritic length (**J**) and total number of dendritic tips (**K**) of neurons in (**F-I**) shows that CRP1 is required for Ca^{2+}-dependent dendritic growth. **A-E**, n = 3, **F-K**, n = 60; * $P < 0.05$, *t*-test; Mean values ± SEM are shown. Scale bar, 50 μm.

Hippocampal neurons at 3 DIV were treated with KCl and expression of CRP1 was determined at different time points (**A**), or 48 hours (**B**,**C**) or 24 hours (**D**,**E**) after addition of KCl.

Figure 7. CaMKIV and CREB mediate the upregulation of CRP1 induced by KCl. (**A**) Inhibitor KN62 of CaM kinases decreases CRP1 mRNA levels. While KN62 decreases the expression of CRP1 under basal condition, KN62 completely blocks the upregulation of CRP1 induced by KCl. (**B**) Inhibitor of MAP kinase, U0126, does not influence expression of CRP1. MAP kinase is not involved in the upregulation of CRP1 mRNA induced by KCl. (**C**) Inhibitor of PKA, KT5720, increases CRP1 mRNA expression. (**D,E**) CaMKIV, but not CaMKII, mediates the upregulation of CRP1. In N2a cells, KCl treatment also increased CRP1 mRNA expression. Constitutively active form of CaMKIV (caCaMKIV) and CaMKII (caCaMKII) were used and only caCaMKIV increased CRP1 mRNA levels (**D**). The ability of CaMKIV to increase CRP1 mRNA levels is further confirmed by showing that a dominant-negative form of CaMKIV (dnCaMKIV) blocks the upregulation effect of KCl (**E**). (**F**) CREB mediates the upregulation of CRP1 mRNA induced by CaMKIV or KCl. (**G-L**) Representative images of neurons cotransfected at 2 DIV with caCaMKIV and either shCRP1 or control shRNA at a ratio of 3:1, then fixed at 5 DIV. (**K**,**L**) Quantification of total dendritic length (**K**) and total number of dendritic tips (**L**) of neurons in (**G-J**) shows that CRP1 is required for CaMKIV-dependent dendritic growth. n = 45; * $P < 0.05$, t test; Mean values ± SEM are shown. Scale bars, 50 μm.

Primary neurons at 3 DIV were treated as indicated and the expression of CRP1 mRNA was examined 24 h later (**A-C**). For **D-F**, N2a cells were transfected with different vectors and the expression of CRP1 was examined 2 days later. The N2a cells were treated with 50 mM KCl 24 hours after transfection and the expression of CRP1 was

examined 24 hours after KCl stimulation. The cotransfection of caCaMKIV and KCREB was done at a ratio of 1:2.

Supplementary figure legends

Figure S1. CRP1 protein is widely expressed in the mouse central nervous system. Different brain regions from adult mouse were used for Western blot analysis. A sample from N2A cells transfected with plasmid expressing CRP1 was used as a positive control. The expression of CRP1 was detected in all of the brain regions studied: olfactory bulb, cortex, hippocampus, striatum, thalamus, cerebellum, brain stem and spinal cord. n = 3.

Figure S2. *In situ* hybridization showed the expression of CRP1 mRNA in neurons in cerebral cortex and hippocampus, and cerebellar Purkinje cells. No significant signal was observed with the sense probe for CRP1 (**A**,**D**,**G**). Neurons in cerebral cortex (arrow in **C**), hippocampus (arrow in **F**), and cerebellar Purkinje cells (arrow in **I**) were positive for CRP1 mRNA. n = 3. Scale bars, 50 μm.

Figure S3. Accumulation of CRP1 was observed at the tips of cultured rat hippocampal neurons. Hippocampal neurons cultured on coverslips coated with laminin were immunostained after 3 DIV. Accumulation of CRP1 was observed at the tips (arrows) of neurons. Scale bar, 50 μm.

Figure S4. Cotransfection of CRP1 and constitutively active Cdc42 (caCdc42) increased the percentage of cells with filopodia. COS-7 cells were transfected with GFP control vector alone (**A**-**D**), or GFP-CRP1 alone, or cotransfected with GFP control vector and myc-tagged constitutively active Cdc42 (**E**-**H**) or cotransfected with GFP-CRP1 and caCdc42 (**I**-**L**). The cells were fixed 48 hours after transfection and stained with actin and myc. (**M**) In COS-7 cells, transfection of caCdc42 alone induced filopodia formation (arrows) in about 10% cells while cotransfection of caCdc42 and CRP1 increased the percentage of cells with filopoda to 18%. n = 3; * $P < 0.05$, *t*-test; Mean values ± SEM are shown. Scale bar, 50 μm.

Figure 1

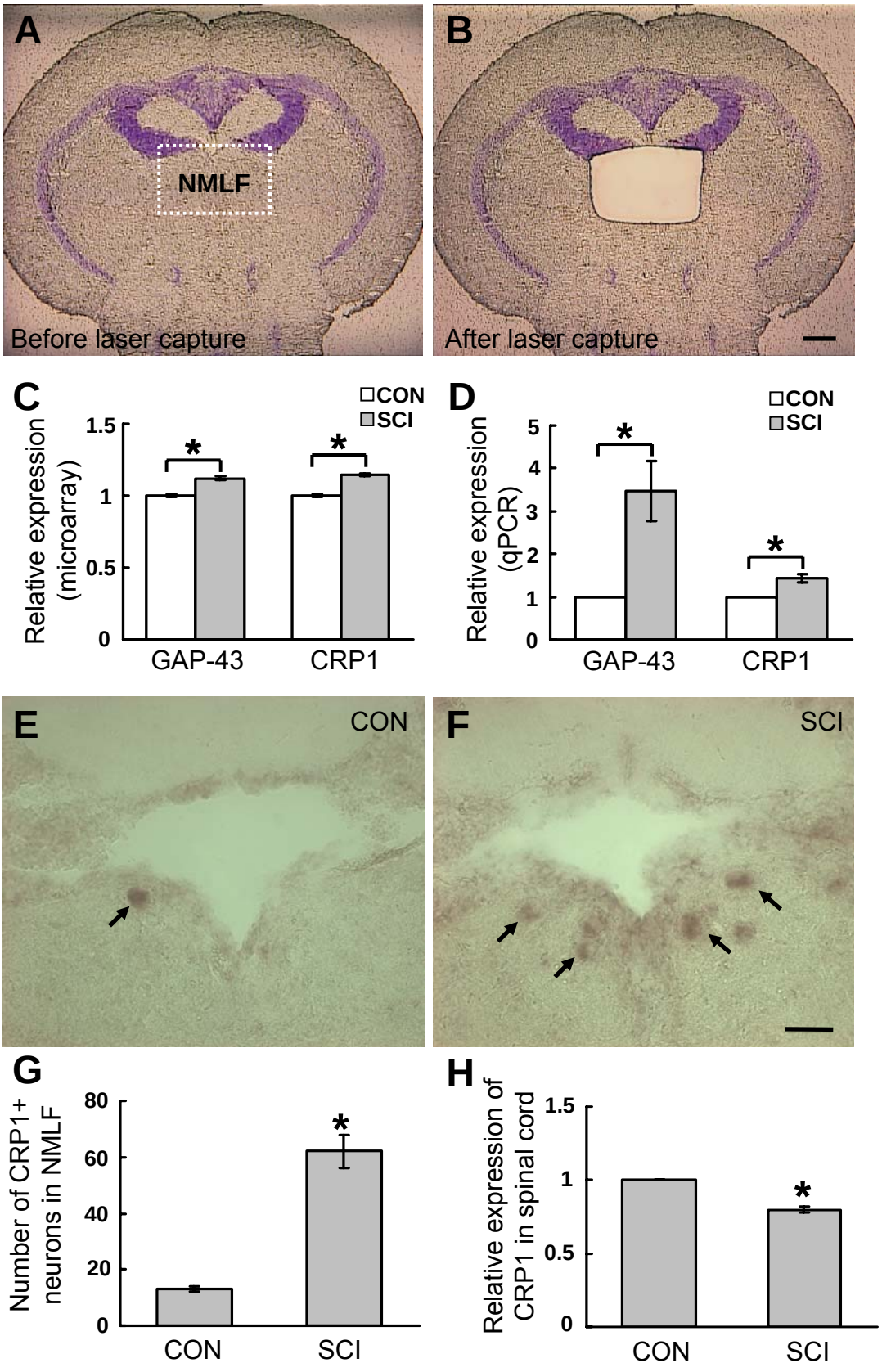
A
NMLF
Before laser capture
B
After laser capture
C
CON
SCI
Relative expression (microarray)
1.5
1
0.5
0
*
*
GAP-43
CRP1
D
CON
SCI
Relative expression (qPCR)
5
4
3
2
1
0
*
*
GAP-43
CRP1
E
CON
F
SCI
G
Number of CRP1+ neurons in NMLF
80
60
40
20
0
*
CON
SCI
H
Relative expression of CRP1 in spinal cord
1.5
1
0.5
0
*
CON
SCI

Figure 2

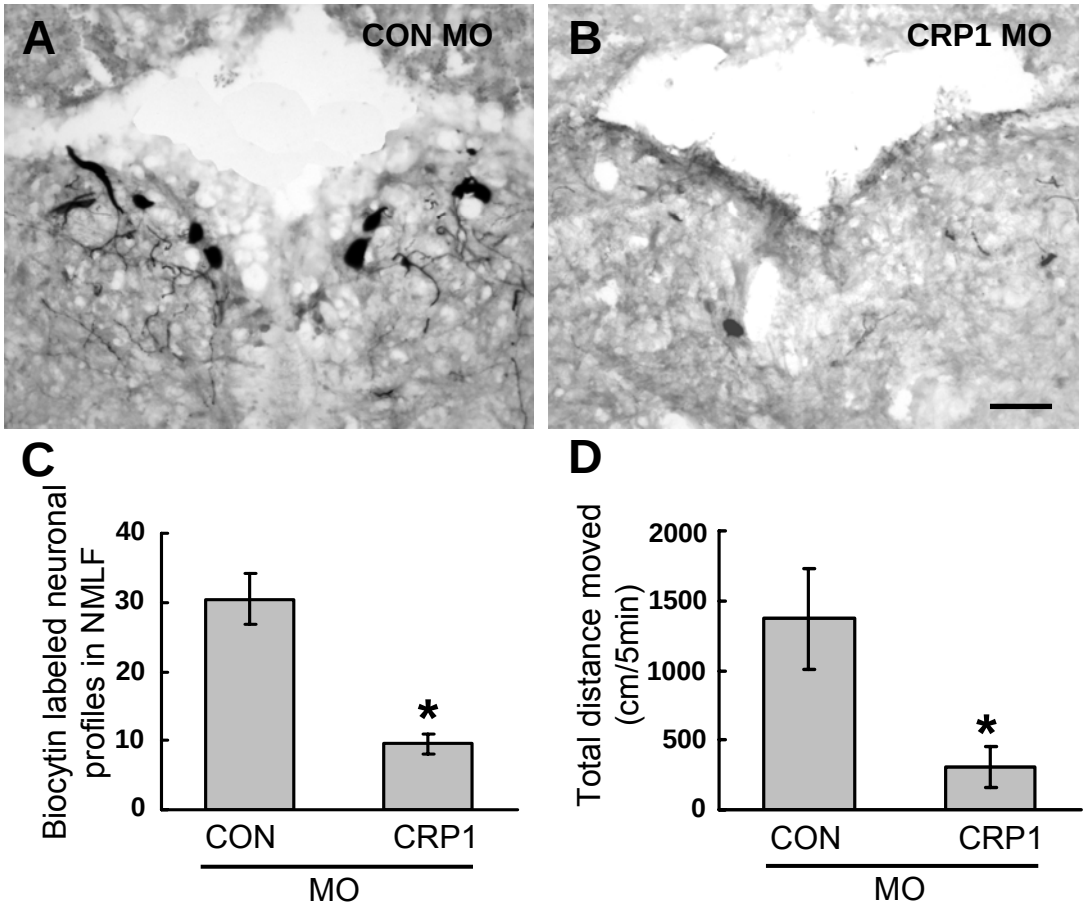
A
CON MO
B
CRP1 MO
C
Biocytin labeled neuronal profiles in NMLF
40
30
20
10
0
*
CON
CRP1
MO
D
Total distance moved (cm/5min)
2000
1500
1000
500
0
*
CON
CRP1
MO

Figure 3

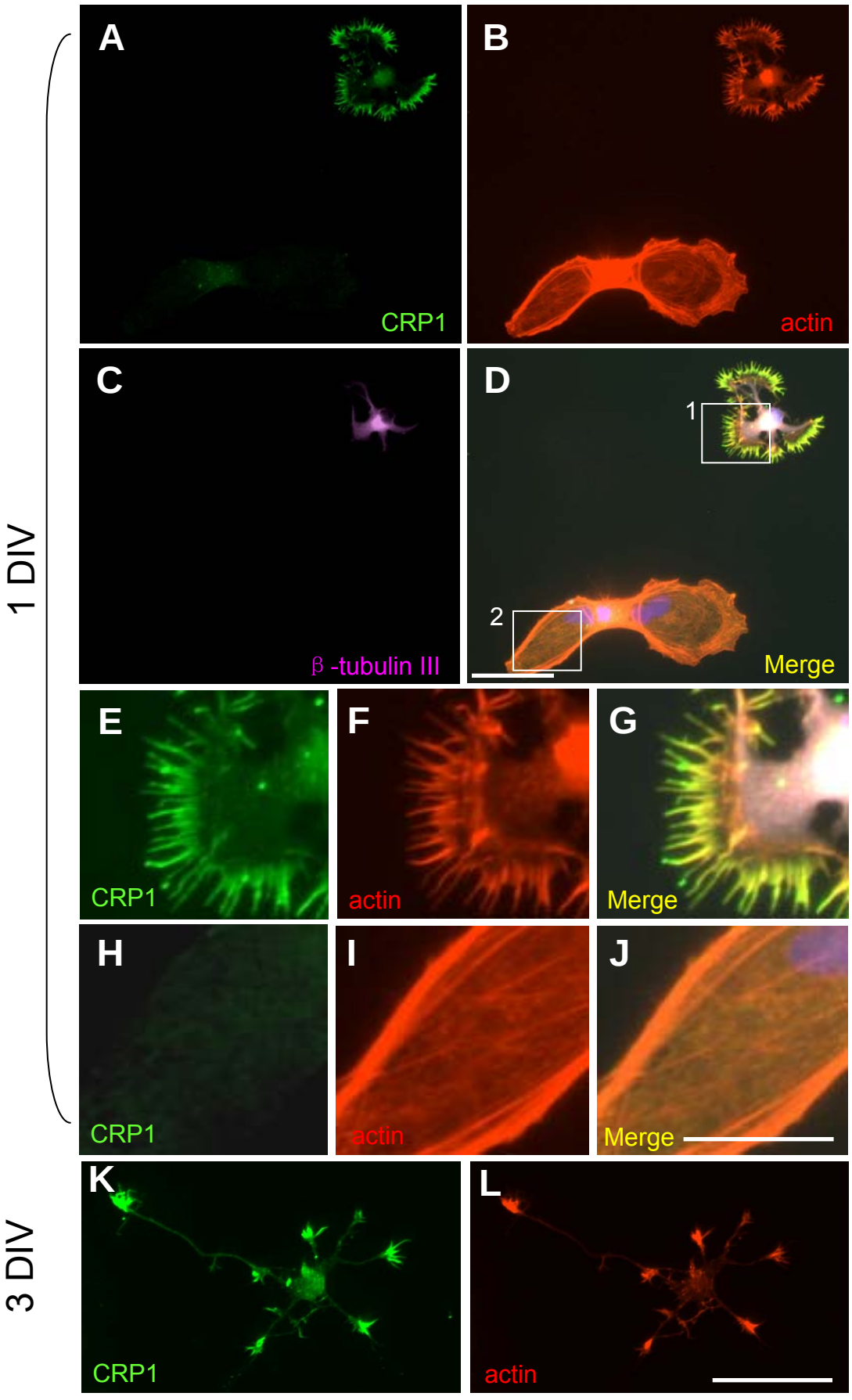
A
CRP1
B
actin
C
β -tubulin III
D
1
2
Merge
1 DIV
E
CRP1
F
actin
G
Merge
H
CRP1
I
actin
J
Merge
3 DIV
K
CRP1
L
actin

Figure 4

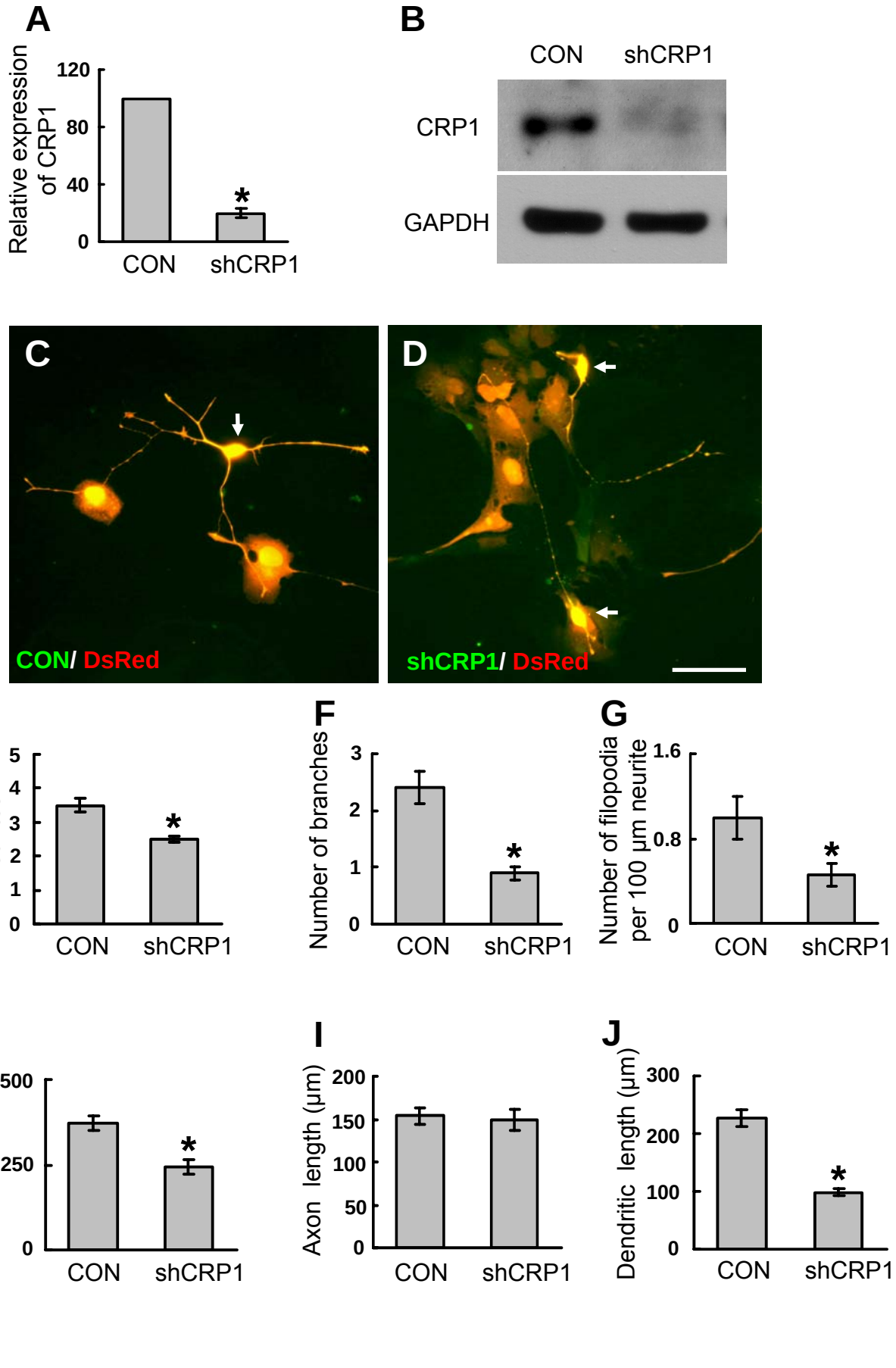
A
Relative expression of CRP1
120
80
40
0
CON
shCRP1
*
B
CON
shCRP1
CRP1
GAPDH
C
CON/ DsRed
D
shCRP1/ DsRed
E
Number of primary neurites
5
4
3
2
1
0
CON
shCRP1
*
F
Number of branches
3
2
1
0
CON
shCRP1
*
G
Number of filopodia per 100 μm neurite
1.6
0.8
0
CON
shCRP1
*
H
Total length of neurites (μm)
500
250
0
CON
shCRP1
*
I
Axon length (μm)
200
150
100
50
0
CON
shCRP1
J
Dendritic length (μm)
300
200
100
0
CON
shCRP1
*

Figure 5

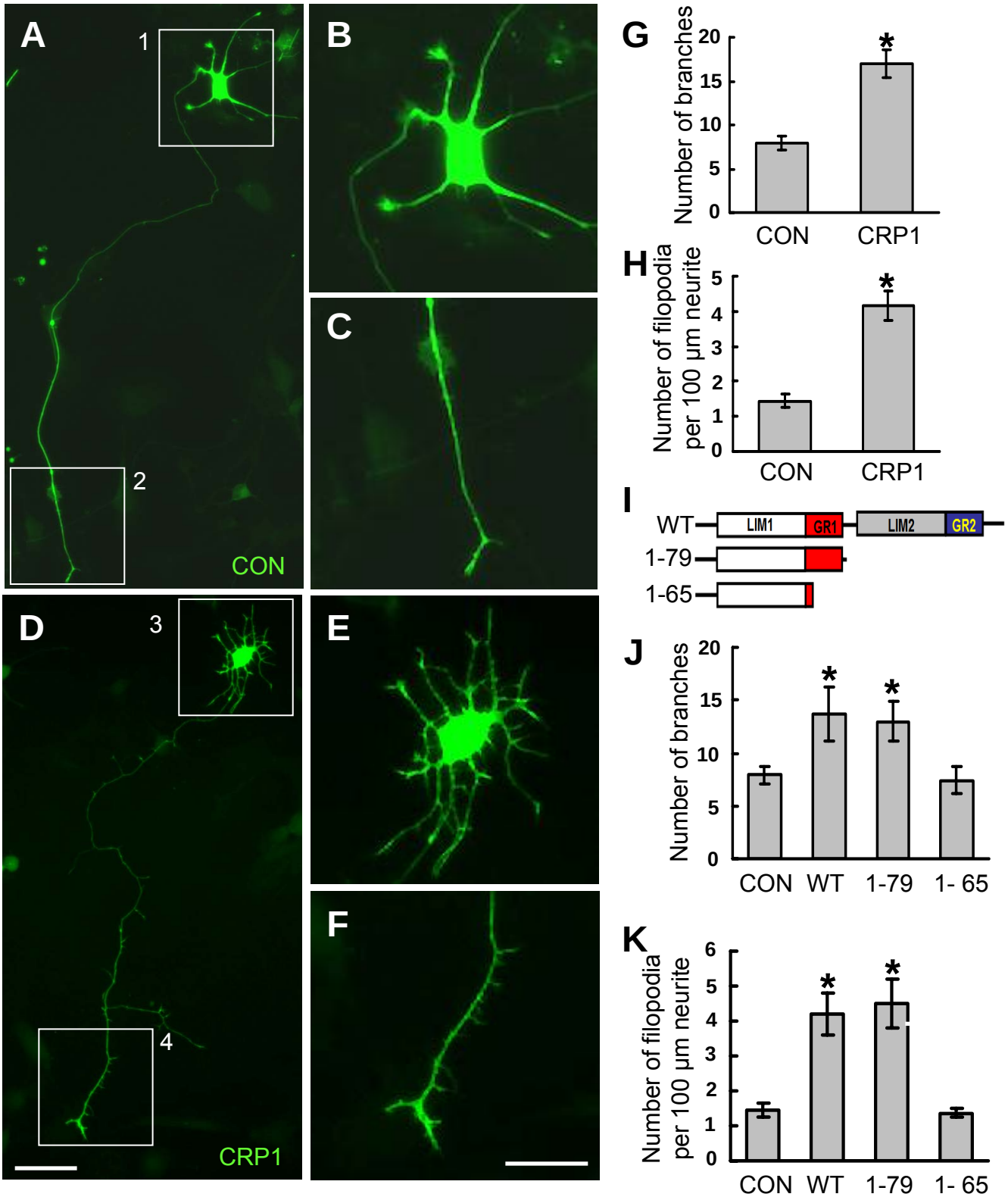
A
1
2
CON
B
C
D
3
4
CRP1
E
F
G
Number of branches
20
15
10
5
0
CON
CRP1
*
H
Number of filopodia per 100 µm neurite
5
4
3
2
1
0
CON
CRP1
*
I
WT
LIM1
GR1
LIM2
GR2
1-79
1-65
J
Number of branches
20
15
10
5
0
CON
WT
1-79
1- 65
*
*
K
Number of filopodia per 100 µm neurite
6
5
4
3
2
1
0
CON
WT
1-79
1- 65
*
*

Figure 6

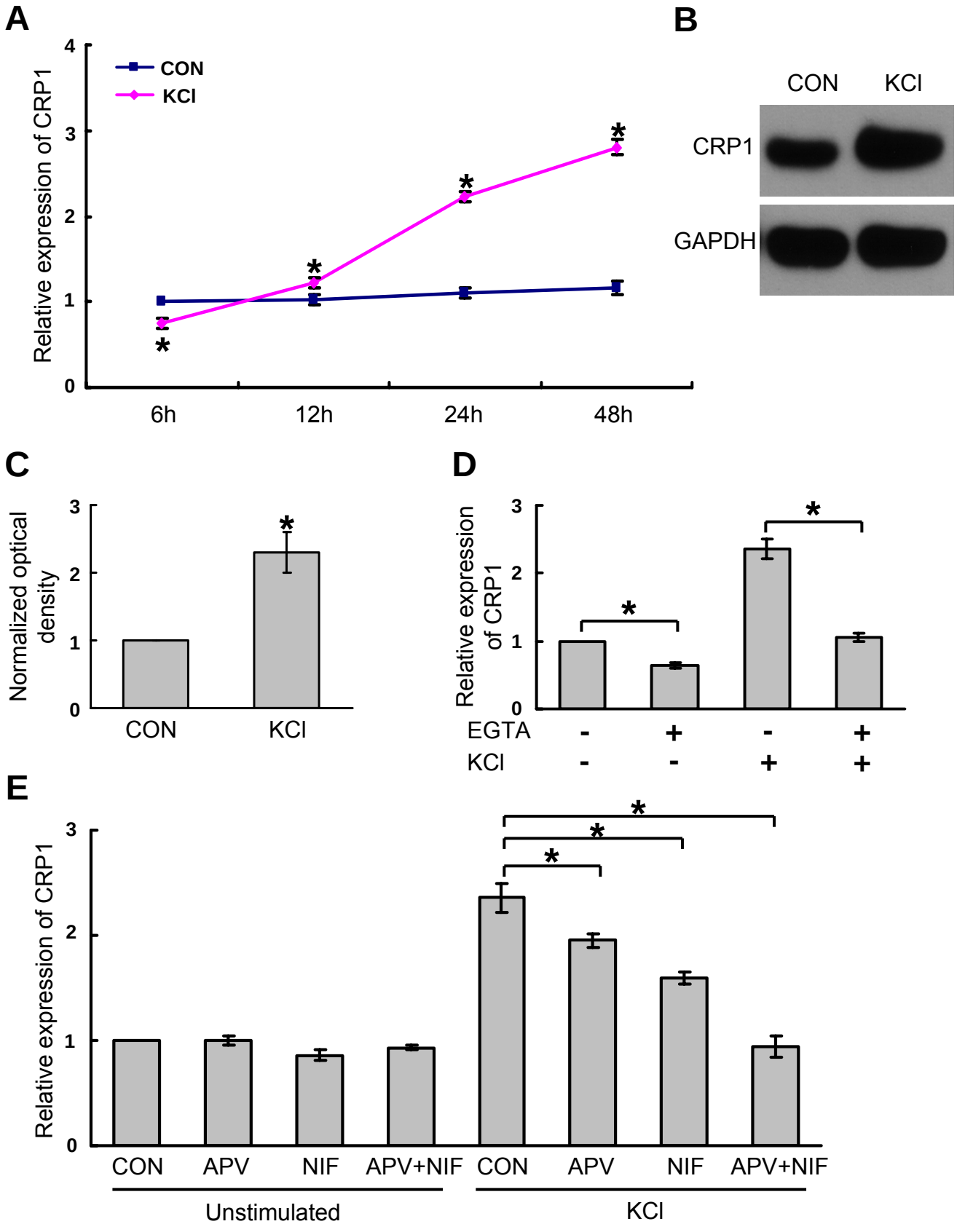
A
B
C
D
E
CON
KCl
Relative expression of CRP1
6h
12h
24h
48h
CRP1
GAPDH
Normalized optical density
EGTA
KCl
APV
NIF
APV+NIF
Unstimulated
KCl

Figure 6 (continued)

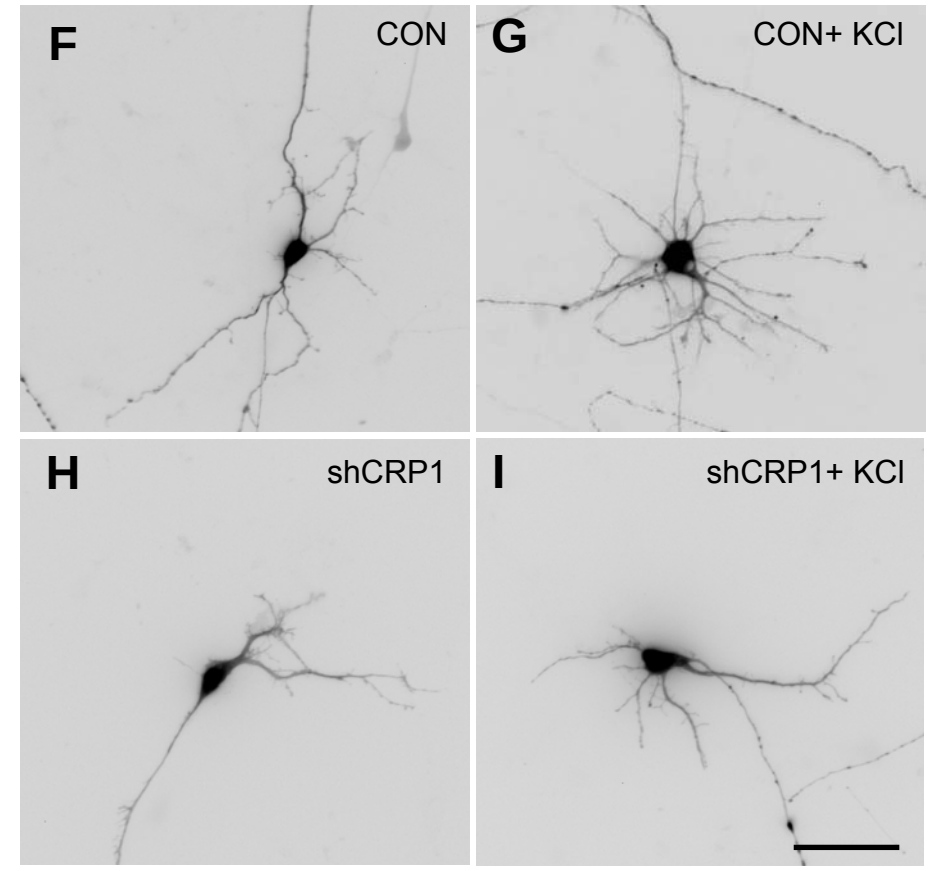

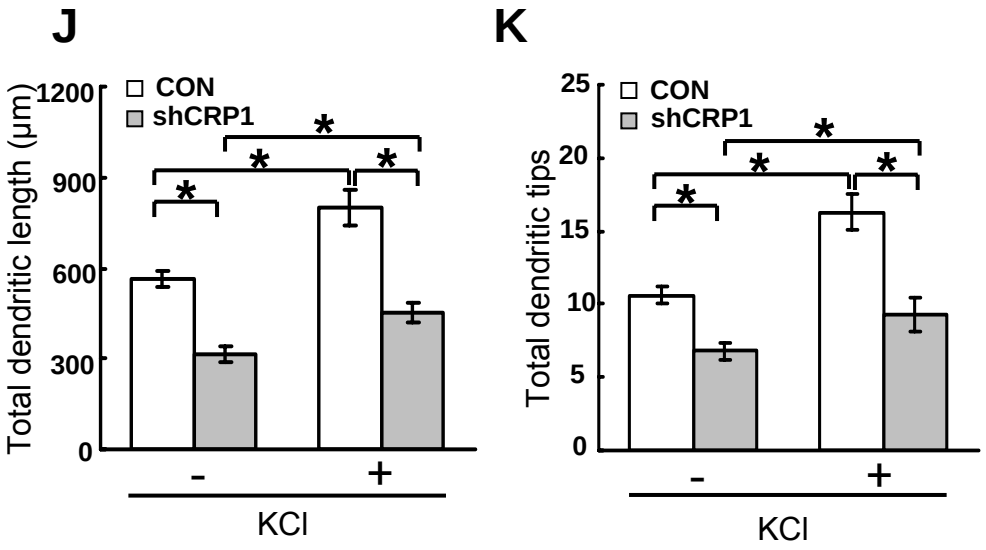

Figure 7

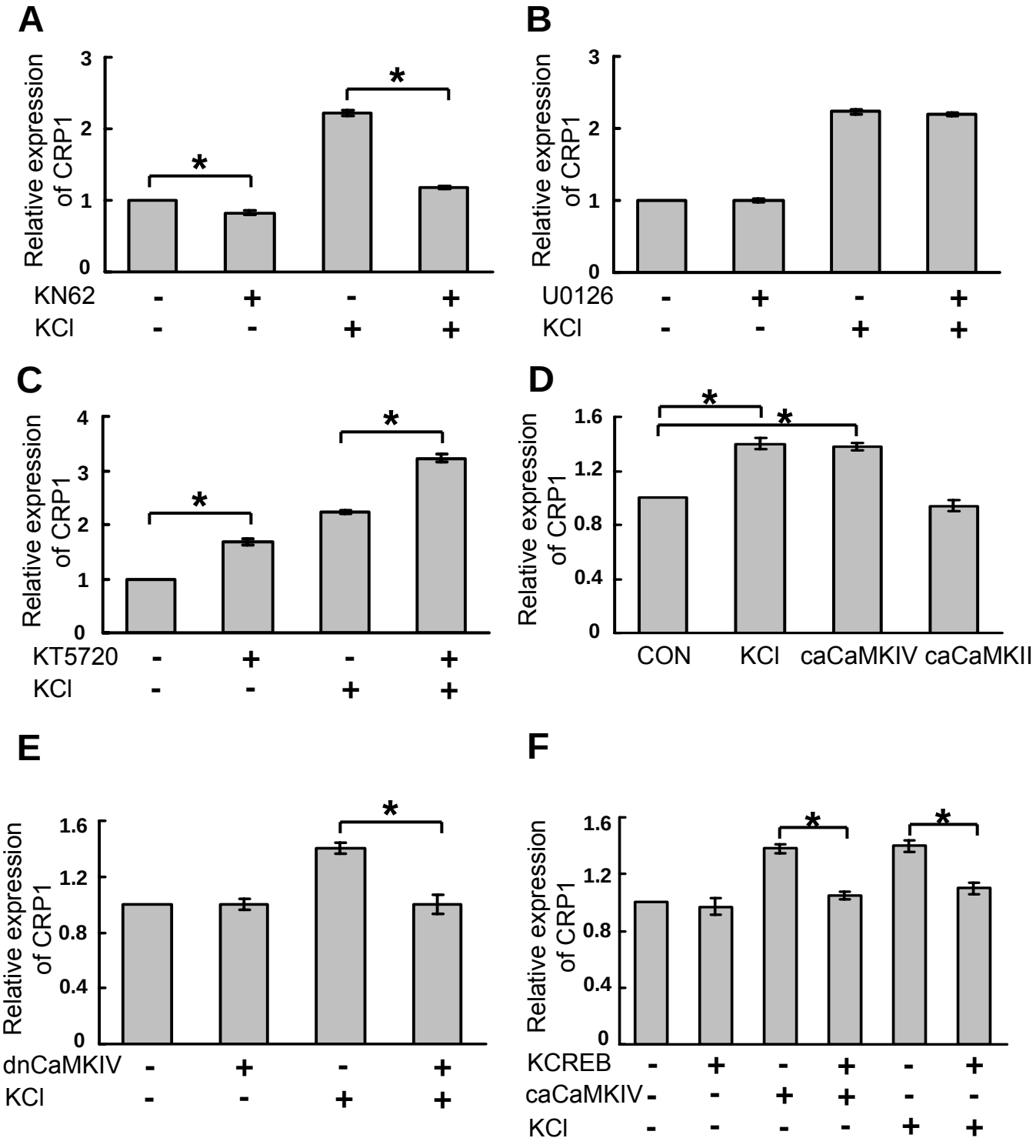
A
Relative expression of CRP1
3
2
1
0
*
*
KN62 - + - +
KCl - - + +
B
Relative expression of CRP1
3
2
1
0
U0126 - + - +
KCl - - + +
C
Relative expression of CRP1
4
3
2
1
0
*
*
KT5720 - + - +
KCl - - + +
D
Relative expression of CRP1
1.6
1.2
0.8
0.4
0
*
*
CON
KCl
caCaMKIV
caCaMKII
E
Relative expression of CRP1
1.6
1.2
0.8
0.4
0
*
dnCaMKIV - + - +
KCl - - + +
F
Relative expression of CRP1
1.6
1.2
0.8
0.4
0
*
*
KCREB - + - + - +
caCaMKIV - - + + - -
KCl - - - - + +

Figure 7 (continued)

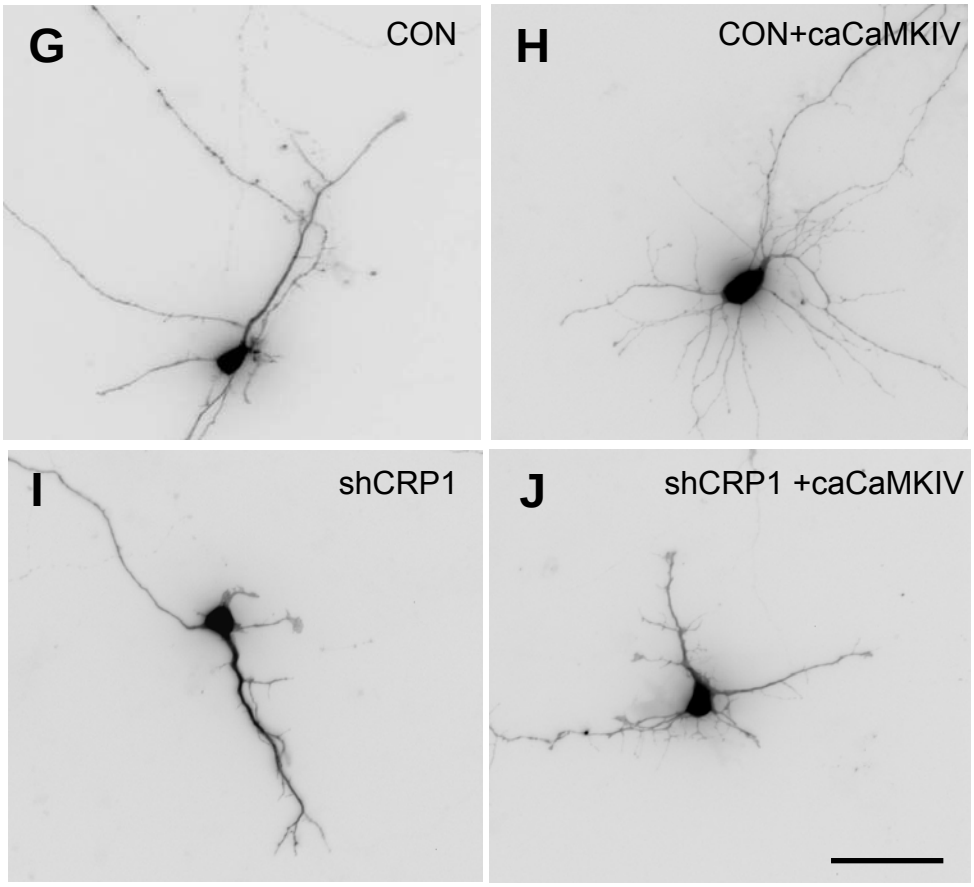

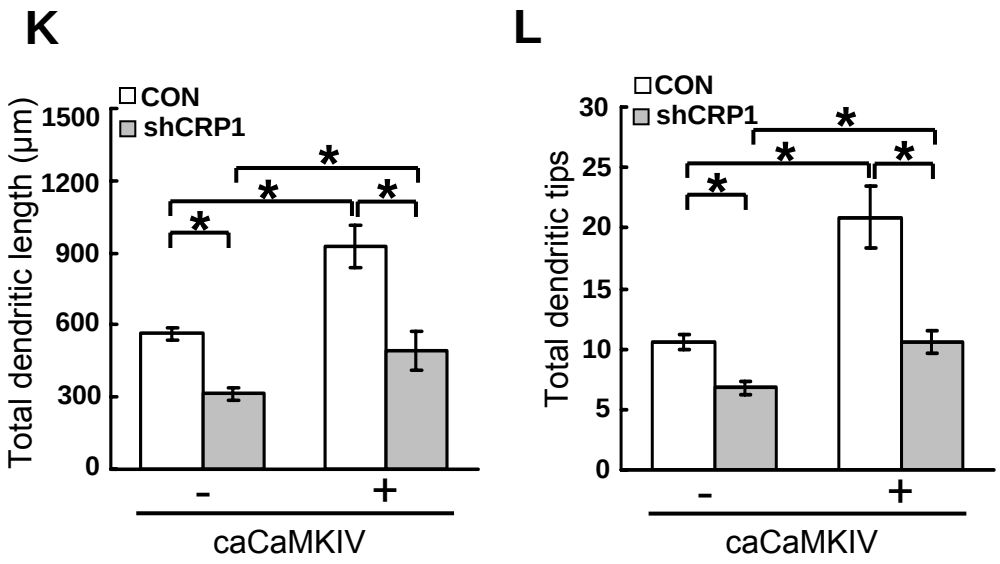

Figure S1

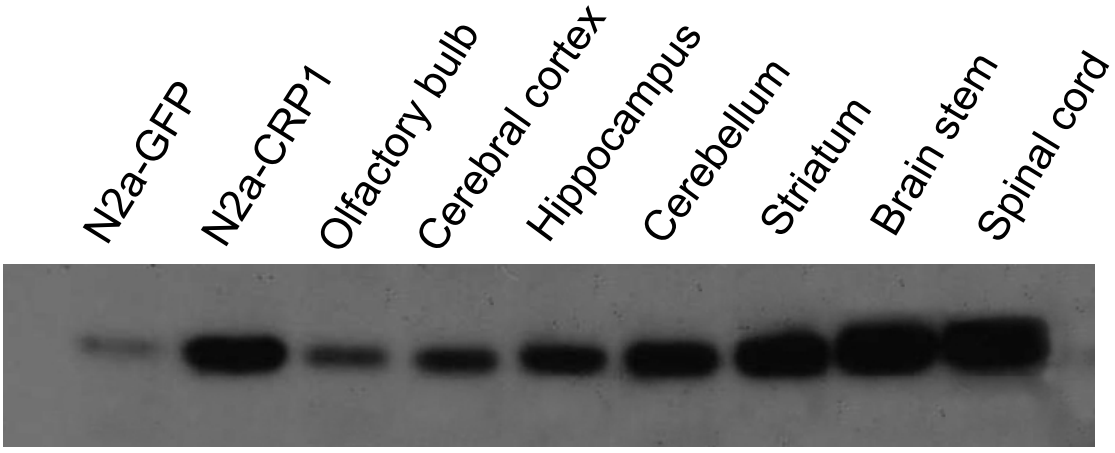
N2a-GFP
N2a-CRP1
Olfactory bulb
Cerebral cortex
Hippocampus
Cerebellum
Striatum
Brain stem
Spinal cord

Figure S2

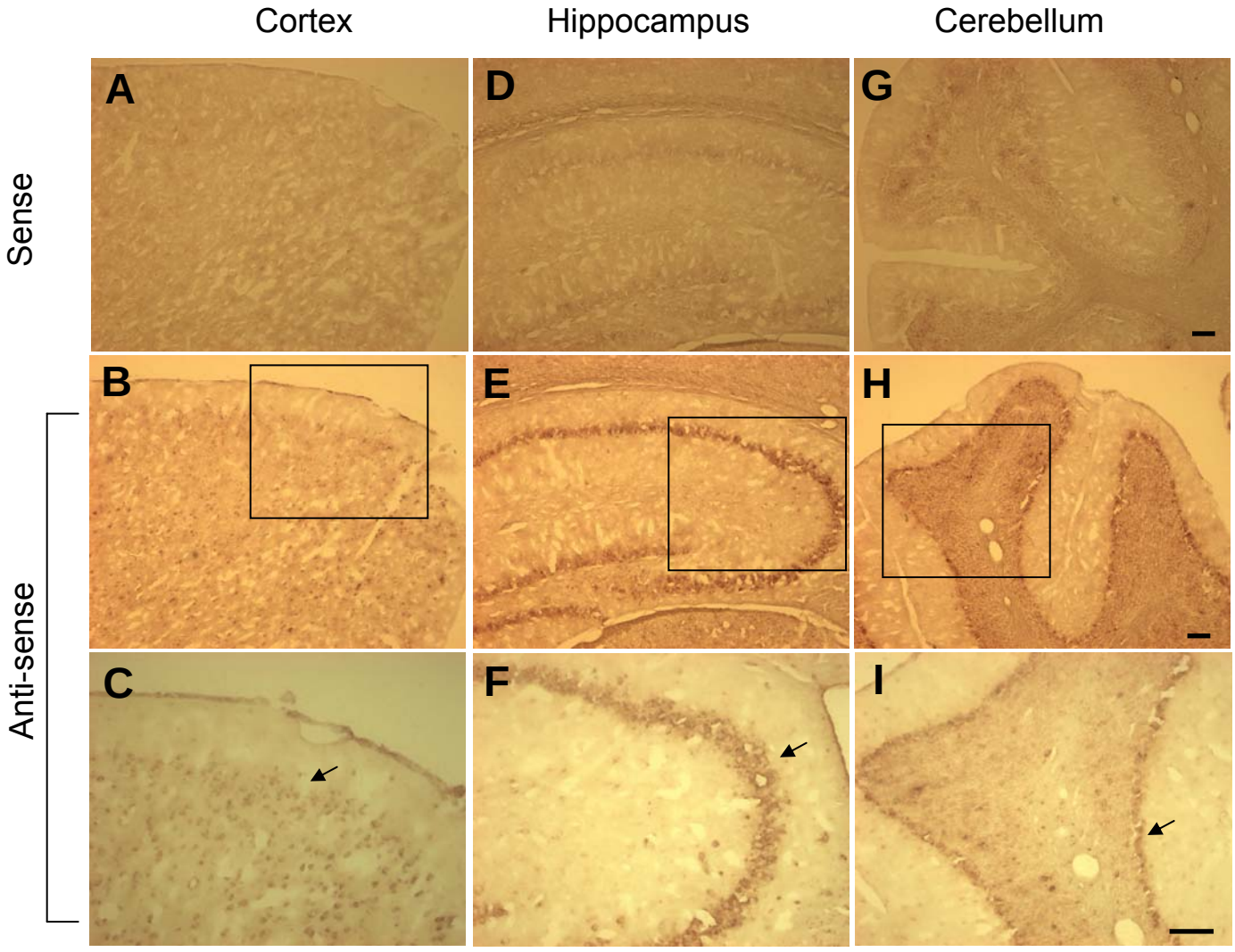
Cortex
Hippocampus
Cerebellum
Sense
Anti-sense
A
B
C
D
E
F
G
H
I

Figure S3

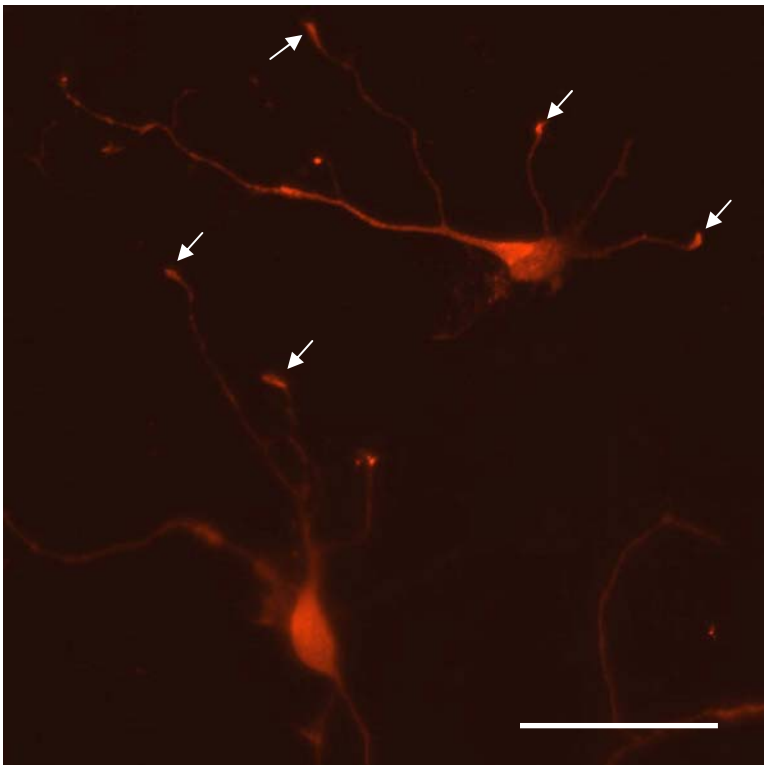

Figure S4

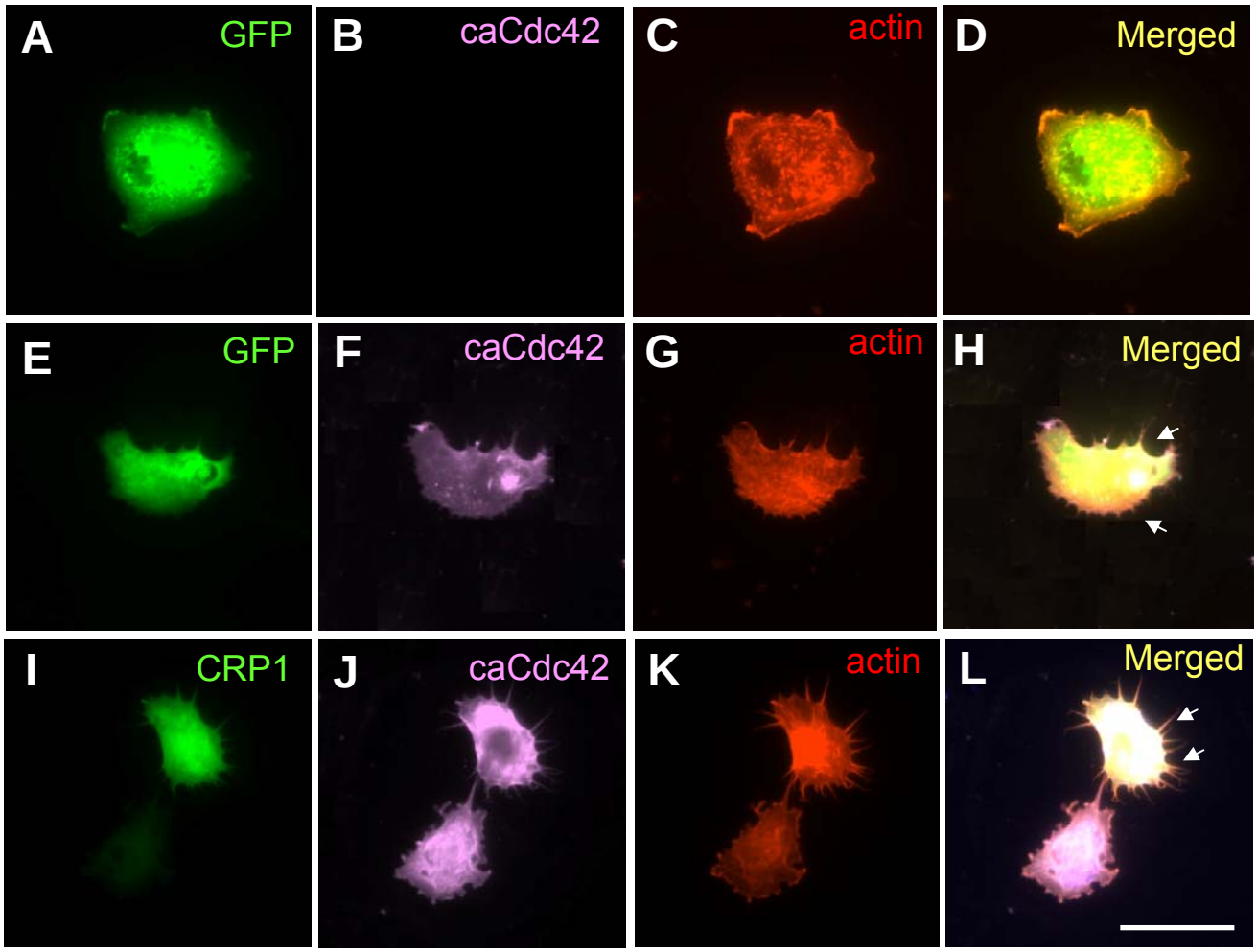
A
GFP
B
caCdc42
C
actin
D
Merged
E
GFP
F
caCdc42
G
actin
H
Merged
I
CRP1
J
caCdc42
K
actin
L
Merged

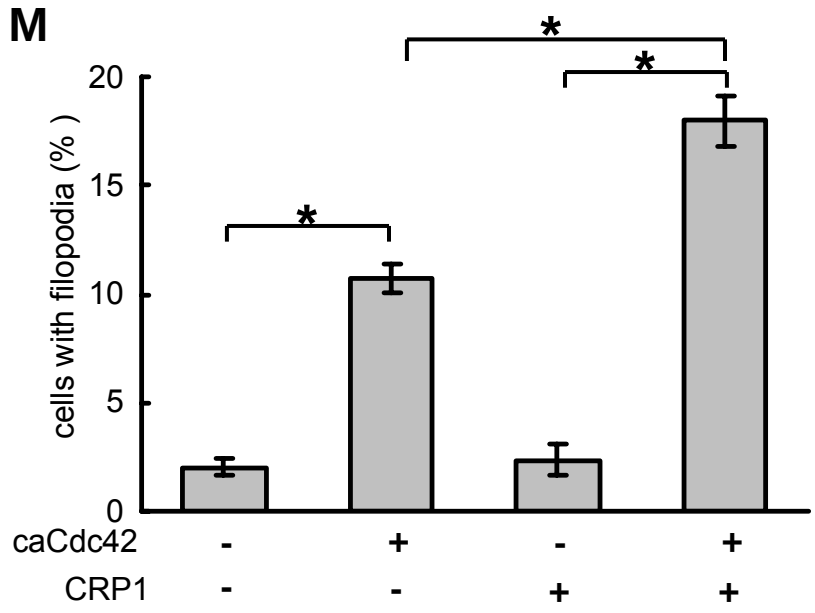
M
cells with filopodia (%)
20
15
10
5
0
*
*
*
caCdc42
-
+
-
+
CRP1
-
-
+
+